

Review

Potential of 3D Printing for Heat Exchanger Heat Transfer Optimization—Sustainability Perspective

Beata Anwajler 

Department of Energy Conversion Engineering, Faculty of Mechanical and Power Engineering, Wrocław University of Science and Technology, 27 Wybrzeże Wyspiańskiego Street, 50-370 Wrocław, Poland; beata.anwajler@pwr.edu.pl

Abstract: In just a few short years, the additive manufacturing (AM) technology known as 3D printing has experienced intense growth from a niche technology to a disruptive innovation that has captured the imagination of mainstream manufacturers and hobbyists alike. The purpose of this article is to introduce the use of 3D printing for specific applications, materials, and manufacturing processes that help to optimize heat transfer in heat exchangers, with an emphasis on sustainability. The ability to create complex geometries, customize designs, and use advanced materials provides opportunities for more efficient and stable heat transfer solutions. One of the key benefits of incremental technology is the potential reduction in material waste compared to traditional manufacturing methods. By optimizing the design and structure of heat transfer components, 3D printing enables lighter yet more efficient solutions and systems. The localized manufacturing of components, which reduces the need for intensive transportation and associated carbon emissions, can lead to reduced energy consumption and improved overall efficiency. The customization and flexibility of 3D printing enables the integration of heat transfer components into renewable energy systems. This article presents the key challenges to be addressed and the fundamental research needed to realize the full potential of incremental manufacturing technologies to optimize heat transfer in heat exchangers. It also presents a critical discussion and outlook for solving global energy challenges through innovative incremental manufacturing technologies in the heat exchanger sector.



Citation: Anwajler, B. Potential of 3D Printing for Heat Exchanger Heat Transfer Optimization—Sustainability Perspective. *Inventions* **2024**, *9*, 60. <https://doi.org/10.3390/inventions9030060>

Academic Editors: Lukasz Orman and Shyy Woei Chang

Received: 27 March 2024

Revised: 10 May 2024

Accepted: 13 May 2024

Published: 16 May 2024



Copyright: © 2024 by the author. Licensee MDPI, Basel, Switzerland. This article is an open access article distributed under the terms and conditions of the Creative Commons Attribution (CC BY) license (<https://creativecommons.org/licenses/by/4.0/>).

Keywords: 3D printing; additive technology; heat transfer; sustainability; heat exchangers; optimization of heat transfer

1. Introduction

The growing energy intensity of national electricity systems is prompting the search for new ways to reduce electricity demand. Energy consumption and pollution are key global issues that require urgent action. Traditional energy sources such as coal, oil, and natural gas are limited and depleting. In addition, their extraction and combustion generate large amounts of greenhouse gases that contribute to climate change. As a result, urban development and technological progress are inextricably linked to appropriate energy management. Effective energy strategies and technological innovation play a key role in shaping a sustainable and future-oriented urban infrastructure. Sustainable energy strategies are approaches to energy management that consider the balance between accessibility, cost effectiveness and environmental impact [1,2]. Such strategies aim to provide sustainable energy access while minimizing negative environmental impacts. Investment in renewable technologies and the development of efficient energy storage systems are key. Improving energy efficiency in various sectors such as industry, transport, buildings, and households can significantly reduce global energy consumption. Finding solutions to global energy and environmental challenges requires international cooperation. Climate agreements, such as the Paris Agreement, are an important step towards global cooperation to reduce greenhouse gas emissions [3]. Educating and raising public awareness about the

need to protect the environment and combat climate change is key to making lifestyles and consumption more sustainable. There is a growing interest in research on energy management and minimizing energy consumption [4].

Solving global energy and environmental problems requires an integrated approach in which governments, businesses, scientists, and the public work together to create sustainable and environmentally friendly solutions.

Sustainable development [5] is an approach to development that meets the needs of the present without compromising the ability of future generations to meet their own needs. This idea implies a balance between the social, economic, and environmental dimensions, taking into account social and global equity. The Sustainable Development Goals (SDGs) are a concrete expression of this concept. The SDGs are a set of 17 goals developed by the United Nations (UN) as part of Agenda 2030. These goals aim to solve global problems such as poverty, hunger, lack of education, inequality, environmental degradation, climate change, social injustice, and others. The answer to the growing challenges of natural resource depletion, climate change, and excessive waste is the circular economy model.

According to the circular economy model [6], the goal is to minimize waste and maximize resource use by keeping products, components, and materials in circulation for as long as possible. In contrast to the traditional linear economic model in which resources are extracted, processed, used, and discarded, the circular economy aims to maintain the value of resources through reuse, recycling, and reprocessing (Figure 1) [7]. Its main goal is to create a more efficient, sustainable, and resilient economic system. One of its key principles is to reduce the amount of waste generated by society. Instead of disposing of products after a single use, it encourages the design and manufacture of items with reuse in mind. The circular economy relies on recycling as a key process. Materials such as metal, glass, paper, and plastic are collected, recycled, and reused in the manufacturing process. It seeks to extend the life cycle of products through repairs, upgrades, and reuse. This supports the efforts to maintain the value of products for as long as possible. It is becoming necessary to implement the concept of sustainable development, the idea of which is the prudent use of resources, and in implementing this idea, energy should be managed prudently, including by reducing its consumption and improving the efficiency of its use.

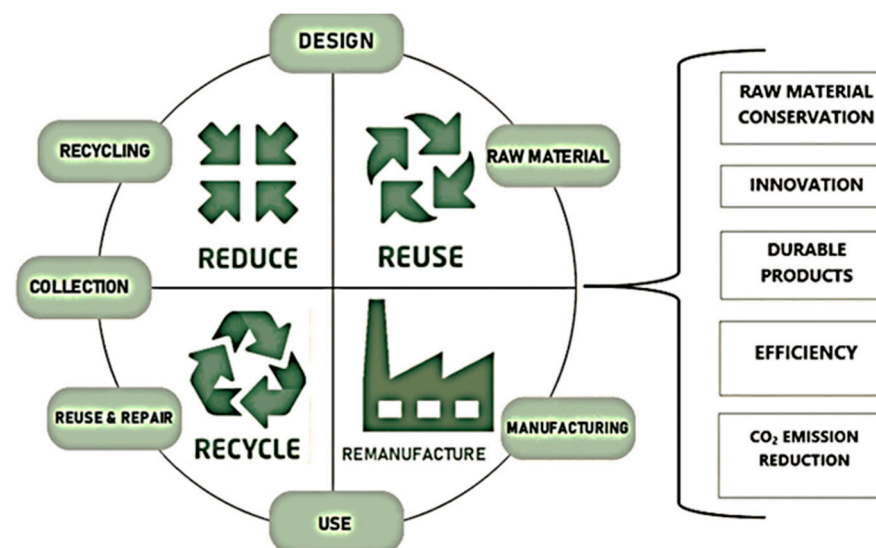


Figure 1. Closed-loop economies. Developed based on [7].

In addition to object manufacturing techniques such as casting, cavity machining, and forming, the incremental technique, also known as additive technology, is of interest from the perspective of this article. This technique involves the application of successive layers of material to form the final finished object. Such techniques have been known about and used

for centuries, for example in construction by applying successive layers of brick and mortar, but today, incremental techniques have also taken on a slightly different form. In this study, we discuss the incremental method of creating a model based on a geometry created in computer software and then manufactured using a numerically controlled machine. This process is also known as 3D printing, while the machines that produce the actual object are called 3D printers.

Additive manufacturing (AM) or printing (3D) is a transformative manufacturing process that enables the creation of three-dimensional objects using various processes and raw materials, typically building a product layer by layer [8,9]. AM can be applied to a variety of materials, such as polymers [10], ceramics [11], metals [12], concrete [13], soil [14] and tissues [15]. Three-dimensional printing is a collective term that encompasses several different technologies. According to ISO/ASTM 52900:2021 [16], there are seven different categories of AM processes (ISO/ASTM International, 2021). According to ISO/ASTM 52900:2021 [16], three categories of AM processes play an important role in this work. These include fused deposition modeling (FDM), selective laser sintering (SLS), and stereolithography (SLA). Stereolithography (SLA) has been characterized as an example of a technology that uses a liquid raw material, the fused deposition modeling (FDM) process of thermoplastics has been selected as an example of a technology that uses a solid build material, and laser powder sintering (SLS) has been discussed as an example of a technology that uses powders [17,18].

Additive manufacturing (AM) has many advantages over traditional manufacturing methods. Some of the key benefits of using additive manufacturing are as follows:

1. Greater availability. Three-dimensional printing can be performed virtually anywhere, as long as there is access to the right 3D printer and raw materials. This allows for more decentralized manufacturing, which is especially attractive to local businesses and communities [19,20].
2. Greater efficiency. Traditional manufacturing methods often waste materials due to the need for cutting and forming. Three-dimensional printing allows materials to be applied precisely in layers, minimizing waste. The 3D printing process can be faster than traditional manufacturing methods, resulting in shorter production cycles [21].
3. Shorter supply chains. AM makes it possible to reduce the need to transport products over long distances and streamline the supply chain by reducing the need for large inventories. Instead, parts can be produced on demand, minimizing inventory costs and waste. This is particularly beneficial for the maintenance of spare parts in the energy industry. Additive manufacturing is widely used in the production of components for renewable energy systems such as wind turbines and solar panels. This includes the manufacture of turbine blades, housing structures, and specialized components that improve the overall performance of renewable energy systems. Local manufacturing helps to reduce transportation-related greenhouse gas emissions [21].
4. Greater design freedom. Three-dimensional printing enables the creation of complex structures and geometries that are difficult or impossible to achieve with traditional manufacturing methods [22,23], thus providing a high degree of customization [24,25]. Lightweight components that can be used in a variety of energy applications, including aerospace, renewable energy, and transportation, thus contributing to improved energy efficiency, particularly in sectors such as aviation and electric vehicles.
5. The ability to easily print replacement parts [26]. Producing custom and complex components tailored to specific energy applications. This is particularly valuable for developing parts for energy systems with unique requirements.
6. Three-dimensional printing often has lower production costs per part, especially for low volumes [27]. Three-dimensional printing facilitates rapid and low-cost prototyping, allowing engineers to test and refine designs faster and more cost effectively than with traditional manufacturing methods. This supports the design and innovation process.

7. New materials with new or improved properties [28,29], such as improved material combinations [30], functionally graded materials [31], and also 4D-printed parts [31,32].
8. The potential of relevant open source technology [33].

Three-dimensional printing represents a new method for the fully automated incremental manufacturing of three-dimensional objects designed as digital files.

Designing for 3D Printing

Additive technology allows for a seamless transition from a digital model to its physical form [34]. One of the main obstacles to the widespread adoption of additive manufacturing is the observed larger-than-expected shape difference between the final print and the intended design [35]. Every 3D-printed object begins as a virtual spatial model (Figure 2). Spatial manufacturing is an integral part of the vision of ‘digital manufacturing’, which is part of a broader industrial trend known as the ‘fourth industrial revolution’ or ‘Industry 4.0’.

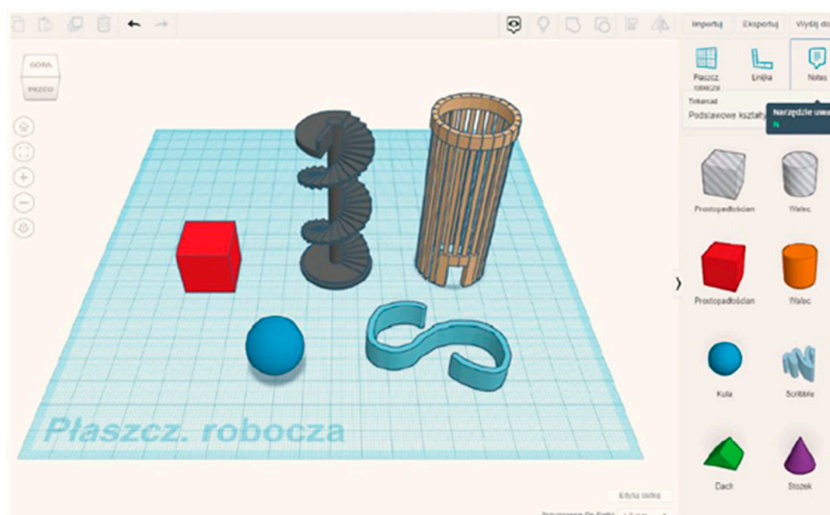


Figure 2. Tinkercad 3D Design Software 101 interface with sample objects placed on the work plane [own design].

The spatial model of the object can be created in any 3D CAD software (Figure 3a) such as AutoCAD Inventor. The next step is to save the object as a mesh geometry (Figure 3b). A mesh geometry is characterized by the fact that it describes only the geometric relationships of the mesh, without information about its color, thickness, or even the unit of length used. The only information relevant to the surface mesh is the coordinates of the vertices of the triangles and the coordinates of the vectors normal to their surfaces [35]. Linear and angular tolerances are important mesh parameters. It is important to remember that a triangulated surface can only approximate the true shape of the surface it describes. Angular and linear tolerances determine the maximum deviation of the mesh from the original interpolated surface. Meshes with low tolerances take up little memory due to the small number of elements. However, these properties come at the cost of significant discrepancies between the generated mesh and the real object [35,36]. In this case, a spherical surface may appear more like a polyhedral surface. For this reason, the aim is to increase the resolution of the mesh to a point where the meshed nature of the wall structure becomes imperceptible due to the accuracy of the model printing technique [35]. Saving the object as a mesh geometry creates a file with an *.stl* extension. Files with the *.stl* extension can also be used in all 3D printing techniques. The finished mesh geometry file can be loaded in 3D CAM software, such as AutoCAD Inventor 2024 which is responsible for locating the object on the work surface and slicing the geometry into layers. The output of the software is a file containing G-code. It is a standard format for writing commands that can be read by the printer

software. The G-code contains the sequence of commands that will be executed by the 3D printer's tooling, although it is not a universal code as it varies from printer to printer. The final step is to load the finished G-code in the software that controls the movement of the printer's actuators. This can be the laser mirror, the extruder head movement or the work surface [37]. The actual creation of the object rests on the shoulders of the 3D printer, with the process varying depending on the incremental technique used. The resulting physical model may require additional processing, such as smoothing edges or cutting off supports. The result is an object that can be used in any way (Figure 4).

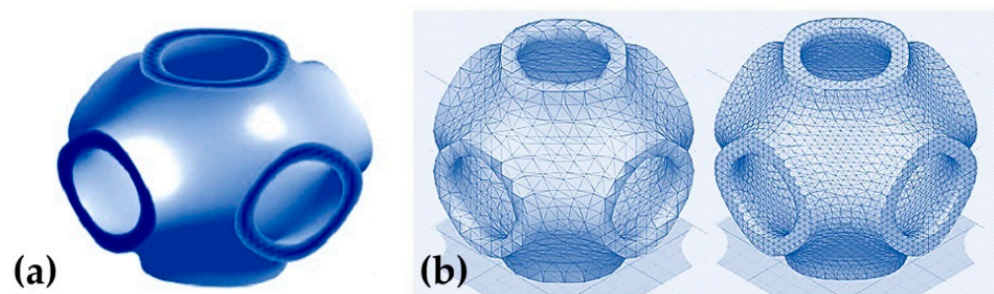


Figure 3. Structure that is a graphical representation of the equation $t = \cos(x) + \cos(y) + \cos(z)$ (a) and surface grid for baseline (left) and densified (right) resolution (b) [own design].



Figure 4. 3D printed part from additive manufacturing [own design].

Referring to the grid resolution in Figure 3b, the effect of grid resolution is visualized. Two meshes were defined at two different resolutions. Note that the file size of the compacted grid is almost four times larger, so it is important to generate grids with a minimum acceptable resolution. In addition, the printing time is also increased. Conversely, for components with large dimensions, the increased production time may not be cost-effective [35]. To address this open challenge, researchers are developing a new collaborative framework that will enable the production of high-quality, large-scale components in a reasonable time. In their studies, the authors of [38–42] used several independent extrusion heads that collaborate to produce the same component. They described a three-dimensional (3D) printing structure that uses a series of mobile robots to apply concrete material to large, one-piece structures. In addition, Zhang et al. [42] used advanced and expensive sensors to prevent collisions between a group of AM machines. A new cutting strategy for the evolving 3D printing platform was proposed by McPherson and Zhou [43]. This involved the collaboration of several mobile MEX machines, where the printing task was split into fragments so that different mobile printers could simultaneously print parts without interfering with each other. In contrast, Bacciaglia and Ceruti [37] proposed an innovative and reproducible methodology for planning the toolpath of a gantry-based multi-head MEX frame, using only the information contained in a traditional G-code file, typical of a dependent multi-head FDM machine. This study describes a strategy for planning and partitioning a single toolpath data file generated by today's standard slicing tools and adapting it to work in a multi-extruder FDM framework. This paper presents pseudocodes describing the innovative methodology and the results of virtual tests on two real large-scale components. By using such an architecture, a large-scale component can be efficiently manufactured at high production rates while maintaining satisfactory quality. Accordingly, the proposed G-code partitioning technique aims to output n separate files depending on the number of available extrusion heads: this is intended to significantly reduce the total printing time.

This article reviews and assesses the potential of 3D printing to optimize heat transfer from a sustainability perspective. This article then presents some key opportunities for heat transfer optimization from a sustainability perspective, the discussion of which has so far not been reflected in the available literature. Key challenges and fundamental research needed to realize the full potential of incremental manufacturing technology are presented. Ultimately, this review offers valuable insights and perspectives, contributing to the discussion on solving global energy challenges through innovative incremental manufacturing solutions.

2. The Promises of 3D Printing to Optimize Heat Transfer

2.1. Better/Worse Heat Transfer Due to Complex Geometries and Internal Structures

Today, 3D printing has become the most powerful technology for rapid design, prototyping, and manufacturing [32]. Three-dimensional printing allows the creation of intricate and complex structures that can maximize surface area and improve heat transfer performance. Custom designs, such as fins and meshes, can be optimized for specific heat dissipation requirements. Complex geometries and internal structures are among the key benefits of 3D printing technology. These features make it possible to create complex and customized designs that are difficult or impossible to achieve with traditional manufacturing methods. Let us take a closer look at complex geometries and internal structures in the context of 3D printing. These materials have a structure consisting of a matrix, which can be solid or flexible, and voids called pores. These porous structures can have different sizes, shapes, and arrangements, giving them different properties and applications [44]. The matrix, which is the solid part of the structure, surrounds and holds the pores. The matrix material can be plastic, metal, ceramic, or any other type of substance. The voids (pores) are areas within the structure that are not filled with matrix material and give the porous structure its characteristic properties. These voids may be isolated or interconnected to form a network of channels. These voids can be filled with various substances such as air, liquid, or phase change materials that can be in solid or liquid states. This saturation affects the thermal, mechanical, and conductivity properties of porous materials. Porous materials containing phase change materials (PCMs) in their structure can be used to store and release energy in thermal processes. Examples of applications for porous materials include thermal insulation, energy storage materials, filters, membranes, and structures for biomechanical purposes. In the field of heat exchangers, porous materials can be used to improve process efficiency, especially in flow control and thermal energy storage [45].

Porous materials can be classified in many ways based on their applications, properties, morphological parameters, materials, manufacturing methods, etc. Here, we base our discussion on the classification presented by [46,47] (Figure 5).

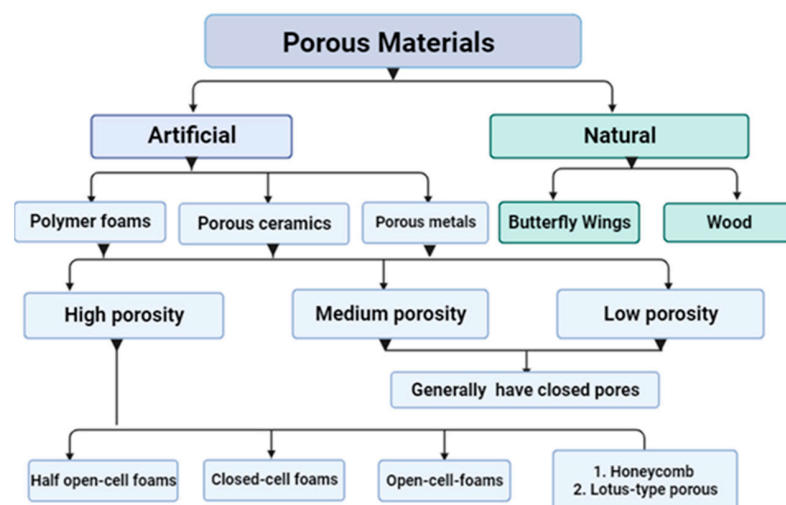


Figure 5. Classification of porous materials. Developed based on [47,48].

Complex Geometries for Better Heat Transfer

Additive manufacturing technology has led to significant innovations in several fields, including heat transfer applications. The capabilities of additive manufacturing (AM) make it possible to achieve complex geometries that would be difficult to achieve using conventional design techniques [49]. In this sense, researchers have taken advantage of this added complexity to explore and develop biomimetic designs inspired by knowledge of ecosystems, organisms, and biological structures [50]. Solutions based on biomimetic designs can provide better energy efficiency and reduce negative environmental impacts. The incorporation of biomimicry can be seen, for example, in the use of cellular or lattice structures, which generally not only have optimized properties of stiffness and lightness but also have good thermal and acoustic properties. An interesting discovery is the generation of spatial structures called minimal surfaces. Minimal surfaces are those that achieve the smallest possible surface area under given boundary conditions. Due to the action of surface tension forces and the desire of the system to seek the lowest energy state, the membrane will occupy the smallest surface out of an infinite number of possible surfaces under given boundary conditions. The structure in question, called a catenoid, represents a broad set of minimal surfaces. Triply periodic minimal surfaces (TPMS) structures represent a subset of minimal surfaces. They are characterized by shape repetition in all three directions along the length of the periodicity. TPMS structures are usually described by trigonometric functions, so it is easy to deduce that the repetition period of the structure depends on the type of function, e.g., for the sine, it will be of the length 2π . The above property makes it possible to duplicate a single block of the TPMS structure many times, while maintaining its continuity at the wall joints. Table 1 below lists some common periodic minimal surfaces, while Figure 6 shows the possibility of combining TPMS structures into larger objects while maintaining surface continuity [51].

Table 1. Summary of the most popular minimum surfaces.



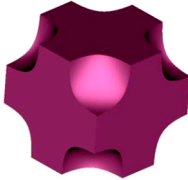

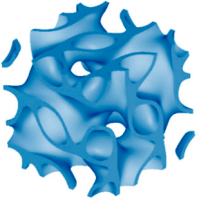
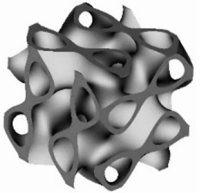
| Names Structures | Equation | Visualization |
|------------------|---|---|
| Gyroid [52] | $\sin(x)\cos(y) + \sin(y)\cos(z) + \sin(z)\cos(x)$ |  |
| Schwarz [53] | $\cos(x) + \cos(y) + \cos(z)$ |  |
| Neovilius [54] | $3 \times \cos(x) + \cos(y) + \cos(z) + 4 \times \cos(x) \times \cos(y) \times \cos(z)$ |  |

Table 1. Cont.

| Names Structures | Equation | Visualization |
|------------------|---|--|
| Diamond [55] | $\sin(x) \times \sin(y) \times \sin(z) + \sin(x) \times \cos(y) \times \cos(z) + \cos(x) \times \sin(y) \times \cos(z) + \cos(x) \times \cos(y) \times \sin(z)$ |  |
| Lidinoïd [54] | $\sin(2 \times x) \times \cos(y) \times \sin(z) + \sin(2 \times y) \times \cos(z) \times \sin(x) + \sin(2 \times z) \times \cos(x) \times \sin(y) - \cos(2 \times x) \times \cos(2 \times y) - \cos(2 \times y) \times \cos(2 \times z) - \cos(2 \times z) \times \cos(2 \times x) + 0.3$ |  |
| Split P [55] | $1.1 \times (\sin(2 \times x) \times \sin(z) \times \cos(y) + \sin(2 \times y) \times \sin(x) \times \cos(z) + \sin(2 \times z) \times \sin(y) \times \cos(x)) - 0.2 \times (\cos(2 \times x) \times \cos(2 \times y) + \cos(2 \times y) \times \cos(2 \times z) + \cos(2 \times z) \times \cos(2 \times x)) - 0.4 \times (\cos(2 \times x) + \cos(2 \times y) + \cos(2 \times z))$ |  |

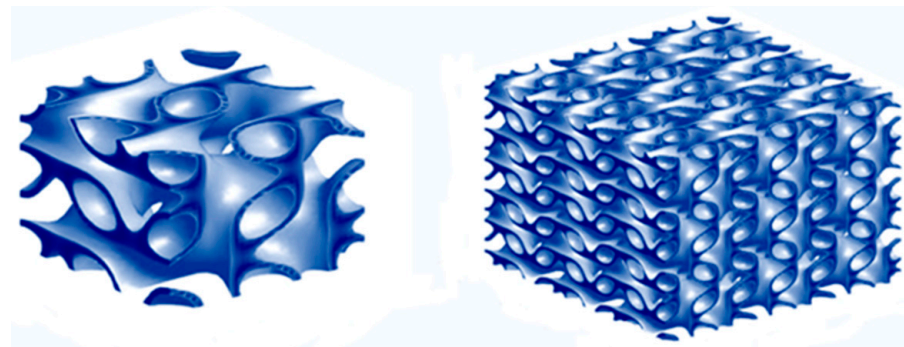


Figure 6. Lidinoïd structure—a single segment with a side length of 2π (left) and the structure formed by duplicating the base segment (right).

Previous studies of AM-made TPMS structures have shown that they have high stiffness, high energy absorption capacity, high strength, no edges, which eliminates areas where mechanical stress can occur, and low weight, all due to their high surface-to-volume ratio (they have localized cross-sectional porosity variation) [56]. Due to the three-dimensional periodicity of the gyroidal network structure, the core of the exchanger creates two identical channels to direct the flow of two separate fluids. As the fluids flow through these channels, heat is exchanged between them as they are in thermal communication. Creating TPMS geometries in CAD is challenging, but as technology advances, minimal surface strategies are becoming more common. There are still too few experimental studies in the available literature to provide an accurate picture of the full application of TPMS structures in heat exchangers. There are mainly numerical studies using CFD to estimate the flow resistance and the heat transfer coefficient when water flows through a channel filled with TPMS. However, these studies clearly show a large variation in the transfer coefficient compared to available heat exchangers with walls made using traditional methods [56,57].

The available literature describes an example CFD study in which Cheng et al. [58] designed an exchanger based on minimal surfaces belonging to the gyroid, primitive, diamond, and Schoen I-WP types. The flow was along a TPMS with the dimensions of $2.54 \text{ mm} \times 2.54 \text{ mm} \times 20.32 \text{ mm}$, for a structure porosity range of $\varepsilon = 20\% \div 80\%$. The researchers found that the higher the Re , the higher the flow resistance, with the lowest for flow along the primitive structure, followed by the gyroid and I-WP, and the highest ($Re = 100$, up to 36 times higher) for flow along the rhombic structure. Analogous to the flow resistance, the value of the Nu number increased successively for the primitive, gyroid, I-WP, and diamond structures. They also showed that the optimal structures were I-WP-based channels, where the thermal efficiency per unit flow resistance was 1.9 times higher than for the diamond channel, and demonstrated that increasing the TPMS porosity value had a positive effect on the Nu number. In another study, Khalil et al. [59] numerically and experimentally investigated forced convection in heat sinks with a structure based on triple periodic minimum surfaces (TPMS), i.e., diamond (D) or gyroidal (G), with a size of 10 mm and a porosity of 80%. Based on their research, they showed that the gyroidal plate structure has the lowest thermal resistance and the highest heat transfer coefficient due to the highest surface density. This work opens the door to designing novel heatsinks for 3D printing and testing their performance in thermal management systems. Another example of research in this field is the study by Raja et al. [60], who presented a water heater connected to a washing machine. This system comprised an electric heater placed in a specially shaped elbow with an internal TPMS (gyroid) structure. The use of the gyroid structure acted as an engineered heat transfer surface and a turbulator for the water flow. According to the authors, they achieved a high efficiency in the implemented design solution. Subsequently, Dixit et al. [61] carried out experimental studies and CFD simulations on a cross-flow heat exchanger based on the gyroid-type TPMS. The actual heat exchange surface consisted of $7 \times 7 \times 7$ elementary structure cells with a side length of 4.6 mm and a relative density of 20% (porosity 80%). The authors showed that, depending on the Re , the value of the heat transfer coefficient was $120\text{--}160 \text{ W}/(\text{m}^2 \cdot \text{K})$, while at the same time recording a 55% increase in the efficiency of the exchanger compared to an exchanger with equivalent thermodynamic properties. In addition, the researchers pointed out that the proposed solution was 90% smaller than a comparable heat exchanger. An example of a heat exchanger study using a TPMS gyroid structure is the work of Reynolds et al. [56], who showed that the gyroid heat exchanger achieved a Nusselt number 112% higher than that of a straight tube control with the same Reynolds number. In addition, it was shown that the overall performance improvement of the TPMS heat exchanger was about 13%. Fan et al. [53] used TPMS (primitive) to cool the battery. Experimental studies and computer simulations (CFD) showed that the maximum temperature of the battery was reduced by about $60 \text{ }^\circ\text{C}$ compared to water cooling in a conventional straight tube.

The limited number of experimental studies reported in the literature suggests the need for further experimental studies to better understand the heat transfer coefficients and fluid flow resistance in contact with TPMS. The optimization of designs with higher heat transfer coefficients requires consideration of the energy required to operate the equipment, which in turn requires flow under conditions of increased flow resistance. Of the many TPMS types available, only four have been subjected to CFD and experimental testing: primitive, gyroidal, diamond, and I-WP. The use of TPMS in heat transfer increases the average Nu value many times over circular or flat surface channels, but also increases the flow resistance. The flow rates in the channels based on TPMS depend, among other things, on the geometry of the TPMS and have the same geometrical parameters (dimensions, number of elementary minimum surface cells, relative density) and flow resistances; the lowest flow resistances were obtained for primitive TPMS, followed by gyroidal, I-WP, and diamond TPMS.

Further exemplary work describing the advantages of developing a working fluid-wall interface (not TPMS) produced by AD techniques has been published in the following papers: [62] (lattice structure); [63] (porous open cell aluminum foam); [64] (compact heat

pipe); [65,66] (heat transfer from tetrahedral Kelvin foam to air); [67] (octet, D-cube, tetrahedral and cube); [68] (longitudinally ribbed tube); [69] (pin fin arrangements in annular channels); [70] (diaphragm); [71,72] (inserts that turbulence the flow of the medium in the tube); and [73] (study of the thermal conductivity of AlSi10Mg formed by melting powder with a bed and modified by heat treatment). The ability to create complex geometries and intricate internal structures using 3D printing has improved heat transfer performance in several important ways. First, the creation of complex surface structures, such as fins and microchannels, can significantly increase the surface area available for heat transfer [74]. An increased surface area allows for better heat dissipation or absorption, depending on the application [48]. Jha et al. [75] designed and tested a microchannel tubular heat exchanger, using high-density microgrooves (with fin widths of 100 μm), designed for absorption refrigeration applications. In both studies, a significant increase in the overall heat transfer coefficient to 10,000 $\text{W}/(\text{m}^2 \text{K})$ was achieved, using water as the resident fluid. Andhare et al. [76] tested a flat plate heat exchanger with a microchannel collector designed for single-phase heat transfer, with equal water flow rates on both sides. As a result of the tests, the authors obtained a total heat transfer coefficient of up to 22,000 $\text{W}/(\text{m}^2 \text{K})$, which is an extremely high value for single-phase heat transfer. Arie et al. [77] investigated an air–water heat exchanger made from titanium produced using a 3D direct laser metal sintering (DLMS) process. They found an increase in heat transfer of 15–50% compared to state-of-the-art heat exchangers equipped with corrugated fins. Tiwari et al. [74] presented the design and described the performance of a compact heat exchanger with a microchannel tube collector. This heat exchanger uses an improved commercially available tube, which has a ribbed structure on the outer surface and a spiral groove pattern (corrugation) inside the tube. Experimental single-phase tests showed an overall heat transfer coefficient of 22,000 $\text{W}/(\text{m}^2 \text{K})$, and the shell side heat transfer coefficient was 45,000 $\text{W}/(\text{m}^2 \text{K})$, with shell side and tube side water flow rates of 82 g/s and 806 g/s, respectively. The researchers showed that the heat transfer coefficient on the shell side was an order of magnitude higher than in the commonly used shell and tube and plate heat exchangers.

Recently, there has been a surge in research into regular metal meshes that can be additively manufactured due to their “potential” to provide multifunctional and tunable heat exchanger properties. Additively manufactured meshes, which differ significantly from commercially available meshes, can result in much higher heat transfer coefficients. Furthermore, the design freedom allows for different porosities to achieve higher effective thermal conductivity. The use of regular meshes in tubular heat exchangers, as wicks in heat pipes, as heat transfer enhancement elements in boiling heat transfer, and as transpiration cooling mechanisms for turbine blades as an alternative to conventional technologies is promising. The flexibility of 3D printing allows components to be tailored to specific heat transfer requirements. Designers can customize structures at the microscopic level to optimize thermal performance for a specific application [48]. For example, the studies by Ho et al. [78] and Ho and Leong [79] on a lattice structure consisting of a rhomboctet unit cell topology in a rectangular block as well as a circular insert configuration showed that these lattices provide significantly higher thermal performance compared to open cell metal foams, conventional pin-fin heat sinks, and spiral inserts. Effective thermal conductivity values for rhombohedral unit cells with porosities of ~ 0.84 – 0.85 were measured to be about 5.5 times higher than those of stochastic aluminum metal foam samples with similar strut diameters. Broughton and Joshi [80] conducted a comparison of the performance of a mesh with a porosity of 0.865, additionally fabricated using DMLS with AlSi10Mg. They found that the regular mesh had a 60% higher heat transfer coefficient, with a $\sim 66\%$ higher pressure drop compared to stochastic metal foams. Liang et al. [54] analyzed the effect of different strut shapes, including circular, rectangular and elliptical, on heat transfer and pressure drop across the face. All strut shapes in cubic meshes had the same porosity (~ 0.92) and were made from epoxy resin using the SLA process. The round strut was shown to have the lowest heat transfer and pressure drop, but achieved the highest thermal-hydraulic performance. The heat transfer through the end wall in the

single cell thickness configuration was three times higher than in the flat channel using FCC meshes. The elliptical and rectangular shapes provided approximately 27–31% and 25–26% higher heat transfer than the circular shape in FCC grids, due to the better mixing and flow acceleration. In conclusion, the optimization of strut shapes with similar cell topologies was shown to improve the performance of lattice heat exchangers.

Three-dimensional printing is particularly beneficial for heat flow optimization because of its ability to create complex structures and custom geometries. Table 2 shows some specific examples of how 3D printing has been adapted for heat flow optimization.

Table 2. Summary of examples of 3D printing adaptation for heat flow optimization.

| Sector | Application | Optimization of Heat Flow | References |
|---------------------------------|---|--|------------|
| Electronics cooling | Heat sinks with complex structure | Microchannels or fins—heat dissipation. | [73,81,82] |
| Aerospace Industry | Components with integrated cooling channels | Internal cooling channels in the aerospace structures of components, improving resistance to high temperatures | [83–85] |
| Production of wind turbines | Optimization of the blades | Optimizing the shape of wind turbine blades to increase efficiency and minimize drag | [86,87] |
| Nuclear Energy | Components for optimizing heat flow in reactors | Internal moderator components for heat transfer improvement in nuclear reactors. | [88,89] |
| Automotive Industry: | Engine Cooling | Designing engine radiators with a more complex structure to increase cooling efficiency. | [90,91] |
| Liquid cooling in electronics | Custom Cooling Channels | Custom cooling channels for liquid cooling systems tailored to specific electronics configurations | [92,93] |
| Production of heat exchangers: | Channel geometry optimization | Design and manufacture heat exchangers with optimal channel geometry that improves heat transfer efficiency | [61,94,95] |
| Heatsink design optimization | Custom radiators with complex shapes | Design heatsinks with custom geometry, tailored to the specific application and mounting space | [96–98] |
| Cooling in the Apparel Industry | Microchannels in textiles | Creation of microchannel structures that improve ventilation and cooling in sports or specialty apparel | [99–102] |

With the ability to customize 3D printing to meet specific design requirements, heat transfer can be optimized in a variety of applications, helping to improve energy efficiency and system performance.

In summary, 3D printing's ability to create complex geometries and internal structures has revolutionized heat transfer applications, offering improved efficiency and customization across a wide range of industries. This technology continues to play a key role in the implementation of thermal management solutions for electronics, aerospace, power systems, and many other areas.

2.2. Selecting Materials

Choosing the right 3D printing materials to optimize heat flow is critical, as different materials have different thermal and mechanical properties. Table 3 shows some examples of materials commonly used in 3D printing that focus on improving heat flow.

Table 3. Summary of example materials used in 3D printing for heat flow optimization.

| Type | Material | Characteristic | Application | References |
|---------------------------|---|---|--|--------------|
| Heat conductive materials | Copper, aluminum, steel | Excellent thermal conductivity | Manufacture of heat sinks or cooling components | [34,103–105] |
| | Graphene | Excellent thermal conductivity properties | Graphene nanoparticles or graphene composites added to other 3D-printed materials to improve their thermal conductivity. | [106–108] |
| Engineering polymers | PEEK Polyetheretherketone | A thermoplastic polymer with high mechanical strength and chemical resistance | Manufacture of industrial components where both thermal and mechanical properties are important | [109–111] |
| | Nylon | Good mechanical properties, relatively light | Production of components where the balance between mechanical strength and thermal conductivity efficiency is important | [112–115] |
| Metallic materials | Aluminum alloy | Lightweight metal with good thermal conductivity | Production of cooling components such as heat sinks | [103–105] |
| | Aluminum with addition of other materials | | Components with special thermal properties | [116] |
| Ceramics | Aluminum oxide | High heat resistance and excellent thermal properties | Manufacturing components that require efficient heat transfer under extreme conditions | [117,118] |
| Hybrid materials | Carbon fiber composites | The lightness of polymers with the high thermal conductivity of carbon fibers | Both thermal and mechanical properties are important | [119–122] |
| | Metal–polymer composites | A combination of thermal conductivity and flexibility | Advantageous in certain applications | [123–126] |

When selecting materials for 3D printing, it is important to understand the requirements of the application and balance the thermal, mechanical, and performance properties. Different 3D printing technologies may require specific materials, so it is also important to consider the availability of suitable materials for a given printing technology. For heat transfer, metal additive manufacturing is a clear choice due to its higher thermal conductivity and temperature capabilities compared to plastics or polymers [34]. In most cases, the main challenge is to minimize metal oxidation, which can prevent layer adhesion due to lower wettability by liquid metals. As a result, metal printers require an inert atmosphere (usually argon), which contributes to their higher cost. The three most common types of 3D-printed metals (considering all applications) are steel/iron-based alloys, titanium/titanium-based alloys, and Inconel/nickel-based alloys [34]. Another developing trend is multi-material additive manufacturing (MM-AM). Powder bed-based SLM printing of composite materials mainly involves the use of two or more types of powders, where one of them acts as a continuous (matrix) phase, while the other acts as a dispersed (reinforcing) phase. [127,128]. More advanced multi-metal printing can be achieved by using deposition-based processes, for example in areas related to thermal management. Oniuke et al. [129] combined IN718 with a copper alloy (GRCop-84), which increased the conductivity by about 300% compared to IN718 alone. Heer et al. [130] fabricated magnetic–non-magnetic bimetallic structures of graded composition using a laser-induced lattice shaping system (LENS). Their results confirm that non-magnetic SS316 can be gradually transformed into magnetic SS430L without the need for a weld.

2.3. Lightweight Design and Geometry Optimization

Lightweight design in 3D printing is particularly important for optimizing heat transfer, especially in cases where component weight affects system performance or in applications such as those related to aerospace, the automotive industry, or power generation. Designing components with open structures, such as lattice structures, allows for lightweight structures while maintaining a relatively high mechanical strength. Regular lattices fabricated using AM technology have received considerable attention from researchers in the biomedical and civil engineering fields [34,131]. Many previous studies have focused on understanding their mechanical response, flow permeability, and fluid-induced shear stress [131].

For example, Kamal and Rizza [132] described an example of an air cantilever that reportedly provides greater stiffness than its traditionally manufactured counterpart, while weighing 15% less. Another example can be found in the work of Bacellar et al. [133], who achieved up to a 50% reduction in size and pressure drop in an optimized air–fluid heat exchanger compared to a basic standard tube system through optimization. In another example, Alshare et al. [134] optimized the flow in an oil manifold to minimize energy loss using CFD numerical analysis; the resulting manifold, manufactured using 3D printing technology, weighed 84% less than the original base model, while reducing the pressure drop by 25%. In one example, Gutmann et al. [135] proposed a 316L reactor for difluoromethylation, where the reactor was wrapped around a serpentine heat exchanger core. Thus, in many industrial heat exchange applications, greater efficiency of the systems will be achieved by combining weight reduction, size reduction, and multitasking (integrated unit operations). In addition to reducing assembly costs, consolidation further increases the efficient use of materials. This means that more material is actively involved in heat transfer. This fact may justify the use of costly, high-performance metals to further improve performance. Additionally, the elimination of assembly will significantly reduce the risk of leaks and other potential failures.

2.4. Localized Production

Localized 3D printing production, especially in the context of heat flow optimization, can bring several benefits from both an economic and environmental perspective. Some of the aspects of localized 3D printing production in the context of heat flow optimization are as follows:

Local manufacturing allows components to be tailored to specific local infrastructure, climate, or specific industrial requirements that may affect heat flow optimization. It eliminates the need for long supply chains, which shortens component delivery times and reduces transportation costs, which is important for sustainability. Shorter transportation distances between manufacturing and application sites reduce the amount of transportation-related waste. Local manufacturing allows for the better customization of components to meet local needs, which can help to optimize heat transfer in specific climatic conditions. It also eliminates the need for the transportation of components over long distances, resulting in reduced logistics costs. It also contributes to better availability of local raw materials and the use of specific materials available in a given region. Local manufacturing makes it easier to comply with local standards and regulations, which is especially important in industries where safety and regulatory compliance are critical. All of this adds up to more sustainable production from an environmental perspective, as it reduces emissions associated with transportation over long distances and energy consumption. There is also the added benefit of stimulating local business and economic development, which is good for the community. Localized production allows for flexibility in adjusting production to meet current needs, which can be especially beneficial in situations where demand for certain components may fluctuate.

Localized 3D printing production in heat flow optimization is therefore a solution that takes into account both economic and environmental aspects while adapting production to specific local conditions.

2.5. Heat Exchangers Using 3D Printing Technology

With increasing environmental awareness and efforts to reduce energy consumption, new generations of heat exchangers need to be more energy-efficient [34]. Improving the efficiency of heat exchangers can help to reduce energy consumption in various sectors such as industry, transportation, and construction [45,74]. Incremental 3D printing (AM) opens up many possibilities for the design and manufacture of heat exchangers (HXs) [136]. Instead of a layout limited to the use of flat or tubular starting materials, heat exchangers can now be optimized to reflect their function and use in a specific environment [132]. Tooling complexity is no longer a limitation, but an advantage. Instead of brazing components, which results in rather inflexible standard components that are prone to leakage, AM finally allows us to create seamlessly integrated and customized solutions from monolithic material [34,131]. The unique advantages of HX with AM technology include optimized geometries with improved surfaces, controlled surface roughness, fully controlled and organized porous structures, and the elimination of welding or soldering [137]. On the other hand, there are several challenges that need to be addressed to fully realize the benefits of AM technology. The introduction of more efficient heat exchangers can benefit from reduced operating costs for heating, cooling, or power generation by using a biomimetic and mathematical approach with parametric modeling. This results in unprecedented configurations and pushes the boundaries of how we should think about heat exchangers today. Investments in new technologies can pay for themselves through lower energy bills and shorter payback periods [131,138–141]. There is a growing demand for advanced heat exchangers that meet the specific needs of various industries. HXs are widely used in the aerospace industry [142,143], the food industry [144], turbine technology [145], chemical processing plants [143], electronic equipment [143,145–148], nuclear power plants [149], solar energy receivers [149], waste heat recovery systems [74,150], building air conditioning [151], heat pipes [64,152,153], and so on. The application of heat exchangers thus ranges from miniature electronic microcircuits to large buildings [34,74]. Table 4 shows some concepts and applications of 3D printing in heat flow optimization related to heat exchangers.

Table 4. List of examples of heat exchangers, heat sinks, or related components manufactured using incremental technology (3D printing).

| 3D Printing | Materials | Advantages | References |
|-------------|--|---|----------------|
| SLM | 316L stainless steel, 6061 aluminum | -The complex ribbed surface of the micro heat exchanger -The exchangers performed consistently. | [154] |
| | | -Experimental determination of the heat transfer characteristics and pressure drops of the four heat sinks. -The study showed an increase in the performance of the studied exchangers. | [155] |
| | Aluminum 6061, stainless steel 316L | -Three heat sinks with a ribbed structure -Better performance than conventional heatsinks -New geometries result in lower pressure drop | [156,157] |
| | AlSi10Mg Ti6Al4V | -Cylindrical geometry for internal channels built at different angles -Surface roughness of internal channels varies with angle of construction | [158] |
| | | -Oil Cooler -Structure will transfer 15 kW of heat under design conditions | [159] |
| | Stainless steel 316, stainless steel 316L | Type 316 stainless steel printed tubes have higher mechanical strength and lower ductility than annealed Type 316L stainless steel. -Oil cooler fabricated. -Unique features include lenticular tubes with offset strip fins and angled plate-fins. | [160] [161] |

Table 4. Cont.

| 3D Printing | Materials | Advantages | References | |
|-------------------|---|--|---|-------|
| DMLS | AlSi10Mg | -DMLS can be used with a new type of alloy to create porous lattice structures. | [162] | |
| | | -Rough surfaces and ribbed surfaces had an average of 63% and 35% better convective heat transfer, respectively, than smooth surfaces. | [147] | |
| | | -Collector–microchannel heat exchanger -The collector–microchannel geometry offers a significant improvement over the state of the art. | [163] | |
| | Titanium alloy | -Air-to-water heat exchangers using a microchannel collector design have shown a 45–100% increase in base conductivity and a 15% increase in heat transfer coefficient for the same pressure drop compared to corrugated surfaces. | [77] | |
| | | -Friction coefficients increased due to the higher ratio of roughness to hydraulic diameter. -Machined channels have relatively comparable thermal performance to grooved channels. | [164] | |
| | DMLS | | -Three samples of corrugated channels, each containing channels of different wavelengths, were designed and additively fabricated to evaluate the pressure loss and heat transfer performance of the channels. | [165] |
| | | | -Cylindrical channels were built in three different orientations, while teardrop and rhombic channels were built horizontally. -Channels built vertically had the lowest coefficient of friction, while channels built diagonally had the highest coefficient of friction. | [166] |
| | | | -A heat transfer correlation is presented that translates the Nusselt number of flow through DMLS microchannels based on predictions or friction coefficient measurements. | [164] |
| | | | -The process of improving the thermal performance of a twisted shell-and-tube heat exchanger using CFD modeling and extended AM fabrication space is presented. -A 40% increase in heat transfer coefficient was modeled. | [167] |
| | | | -Oil cooler -The weight and volume of the heat exchanger is 66% and 50% less, respectively, than a fuel-cooled oil cooler of similar capacity and performance. | [168] |
| | Stainless steel, titanium alloy, aluminum | -Three prototype air-to-water heat exchangers in a power plant -Improved gravimetric heat transfer density compared to a corrugated fin heat exchanger. | [169] | |
| LPBF | | -Bare tube heat exchanger. -Achieves a ~20% reduction in size, a ~20% reduction in air pressure, a ~40% reduction in material volume, and a ~2% reduction in surface area compared to a micro-channel heat exchanger. | [133] | |
| | | -L-PBF used to fabricate a Ti-6Al-4V multilayer oscillating heat pipe (ML-OHP) -The thermal performance of ML-OHP is characterized. | [170] | |
| Wire-Arc Spraying | | -Dense 625 alloy was deposited on the surface of 10 pores per inch (PPI) and 20 PPI nickel foam sheets to produce compact heat exchangers. | [171] | |

Table 4. Cont.

| 3D Printing | Materials | Advantages | References |
|-------------|--|---|------------|
| | | -The 20 PPI foam exhibited higher flow resistance and heat transfer than the 10 PPI foam due to its smaller pore size and larger internal surface area. | [172] |
| | | -The effect of changing the fin height and density of the pyramidal fins has been studied. -Increasing the height or density of the fins also increases the overall thermal conductivity at the expense of higher pressure drop. at the expense of higher pressure drop. | [173] |
| | | -Two new fin geometries were created; pyramidal and trapezoidal. -The two new geometries have better heat transfer performance than traditional rectangular fins, but higher pressure drop. | [174] |
| CGDS | aluminum nickel stainless steel 34 | -Pyramidal rib arrays were fabricated with varying volume fractions of aluminum and alumina. -The use of aluminum-alumina powder as an alternative to pure aluminum eliminates the need for expensive polymer nozzles that wear out quickly. | [175] |
| | | -Produces near-net-shape pyramidal fin arrays in a variety of materials, including aluminum, nickel and Class 34 stainless steel. | [176] |
| | | -Pyramidal Ribs -Classic double recirculation and flow bypass structures observed in areas of trailing ribs. | [177] |
| | | -Pressure drops and convection coefficients for square, round, and diamond fins. -Alternating configurations produce higher convection coefficients and higher pressure drop.. | [178] |
| LIGA | | -The cross-flow micro heat exchanger was developed to provide a function similar to that of a car radiator. -The micro heat exchanger demonstrated a good ratio of heat transfer rate to volume. | [179] |
| LPW | | -Air-to-water heat exchanger -The polymer heat exchanger required 85% less weight but 35% more volume than a corrugated metal heat exchanger of the same capacity. -COP increased by 27%. | [126] |
| | | -Microfluidic channels in the fins of the liquid-liquid heat exchanger. -The walls, which were 0.032 mm to 0.1 mm thick, could be carefully cleaned, but they deformed slightly under pressure. | [180] |
| Polyjet | | -Air-water heat exchanger. -The thin wall (150 μm) reduces the thermal resistance of the wall to only 3% of the total thermal resistance. | [181] |
| FDM | | -Air-to-water heat exchanger -Improving the thermal conductivity of the printed polymer directly affects the performance of the heat exchanger, but the relationship is non-linear. | [182] |
| | | -A polymer composite heat exchanger called a belt-and-tube heat exchanger. -The design is shown to perform similarly to a plate-and-rib heat exchanger, but uses less material. | [183] |

Table 4. Cont.

| 3D Printing | Materials | Advantages | References |
|-------------|-----------|--|------------|
| LOM | | -Complex ceramic heat exchangers can be built using LOM processes. -The ceramic heat exchanger can be manufactured at a reasonable cost. | [184] |
| LCM | | -The creation of complex designs using LCM was demonstrated. -Components with over 99% post-sinter density were obtained | [185] |
| | | -LCM has enabled the production of alumina and zirconia components. -A heat transfer area of more than 3500 mm ² and holes as small as 0.2 mm in diameter can be achieved. | [139] |

Three-dimensional printing for heat flow optimization in heat exchangers and cooling systems opens up new design possibilities that can lead to more efficient and customized solutions compared to traditional manufacturing methods.

2.6. Integration with Renewable Energy Systems

The energy transition is one of the greatest challenges facing our society. To ensure a smooth transition to a sustainable future energy scenario, various technologies need to be developed and implemented. Among the most important options for energy generation are solar cells or windmills and chemical storage in batteries, supercapacitors, and hydrogen. New production methods based on additive manufacturing increase the potential to achieve the highly efficient and intelligent technologies needed to make clean energy technologies more competitive with fossil fuels. In this context, this roadmap highlights the enormous potential of 3D printing as a new way to fully automate the manufacture of energy devices designed as digital files [186]. Integrating 3D printing with renewable energy systems to optimize heat flow opens up a number of opportunities for designing efficient and sustainable solutions. Table 5 presents several concepts and applications of this integration.

Table 5. Summary of the main 3D printing materials and technologies for the analyzed applications.

| Application | 3D Printing | Materials | Reference |
|------------------------------|--------------------|--|-----------|
| Fuel cells and electrolyzers | SLA, EFF, DIW | Electrode materials, stabilized zirconium electrolytes (lanthanum-based perovskite oxides and nickel-based composites), glass sealants | [187–195] |
| | DIW, SLS | Polymer electrolytes (nafion) and electrodes (precious metals), metallic metallics (stainless steel) | |
| Solar cells | DIW, R2R, IL | Current collectors (silver, copper, tin, indium), carriers (polymers), cells (P3HT: PCBM, organic perovskites, CIGS) | [196–204] |
| Thermoelectric cells | EFF, DIW, SLS, SLA | Bi2Te3, BiSbTe, Cu2Se, PbTe | [205–213] |
| Batteries | DIW, EFF | Polymer electrolytes (PVDF-co-HFP), electrodes (LiFePO4-LPF, Li4Ti5O12-LTO, graphene oxide composites) | [214–223] |
| Supercapacitors | DIW, EFF | Polymer electrolyte (KOH/ polyvinyl alcohol), electrodes (activated carbon, Ti3C2Tx MXene nanosheets, manganese dioxide nanowires, silver nanowires, and fullerene), current collector (Ag nanoparticles), package (polypropylene) | [224–232] |

Table 5. Cont.

| Application | 3D Printing | Materials | Reference |
|--|-------------------------|---|-------------------|
| Rotating Machines | DED, SLS | Ti alloys, Ni-based superalloys, high-temperature Fe-based alloys, Ti or Fe-based intermetallic materials | [233–237] |
| Chemical reactors | DIW, DLP, EFF | Reactor (stainless steel, aluminum oxide), catalyst carrier (metal oxides), catalyst (precious metals) | [238–244,244,245] |
| Solid-state refrigerators | SLS, DED, EFF, DIW, SLA | Ferroelectric/ferromagnetic/ferroelastic caloric materials | [246–253] |
| CO ₂ capture and separation | SLS | Metals or alloys with high thermal conductivity (Aluminum AlSi10Mg) | [254–260] |
| Electronics Cooling | SLS | Metals or alloys with high thermal conductivity (Al-Si10Mg, Al 6061, CuNi2SiCr) and polymer composites | [261–267] |

3. Challenges of 3D Printing Technology in the Context of Sustainability

Three-dimensional printing plays an important role in several aspects of the energy sector. Three-dimensional manufacturing is an integral part of the vision of digital manufacturing, which is part of a wider industrial trend known as the fourth industrial revolution, or Industry 4.0. Three-dimensional printing is an inherently more sustainable process as it builds material layer by layer, reducing material waste and energy consumption [37,44,268]. Incremental manufacturing has evolved from a tool that was originally used for prototyping into a key technology for producing functional parts that are used in an increasingly wide range of fields, such as aerospace and medicine [35,36,269–272]. Leading aerospace sectors are using AM technology to produce wind tunnel models, UAVs, engine components, flight test parts, unmanned aerial vehicles, wall panels, metal structural components, and air ducts, illustrating just some of the many possibilities [37]. The design freedom offered by additive manufacturing allows engineers to explore innovative and optimized designs that may not be feasible using traditional manufacturing methods [265]. An example of this is the use of a TPSM gyroid structure in heat exchangers [61], where a Nusselt number 112% higher than the control of a simple tube at the same Reynolds number was achieved. A good example is also the air-to-water heat exchanger made from titanium, produced using the 3D direct laser metal sintering (DLMS) process, where an increase in heat transfer of 15–50% was observed compared to the latest heat exchangers equipped with corrugated fins [142]. This can lead to more efficient and effective energy systems. Additive technology enables the use of advanced materials, including high performance alloys and composites. This opens up new opportunities to create components with improved properties such as increased strength, heat resistance, or conductivity. Traditional manufacturing methods often generate significant amounts of waste [262,264]. Despite this, existing unresolved issues continue to prevent AM from becoming a mainstream manufacturing technique in an industrial context. The main limitations of 3D printing are mainly the anisotropic properties of the final product material, limited material resources, lengthy certification procedures (if any), high raw material prices, the cost of production in large quantities, and the lack of repeatability and reproducibility. In the traditional approach, large-scale objects are defined as those with at least one of the three dimensions exceeding 1 m [273].

Recent advances in adapting 3D printing for energy and environmental applications provide a competitive advantage by improving productivity and product flexibility and reducing costs, which will contribute to industry breakthroughs [274,275]. Methodologies such as continuous and high-speed printing have increased the speed and efficiency of 3D printing, enabling the rapid production of objects. It is also important to adjust printing parameters such as temperature, print speed, and fill density to reduce energy consumption and optimize the printing process. Modern technology has also enabled multi-material and multicolor printing, making it possible to create complex and practical designs in a

single print. The use of hydropower and renewable electricity can temporarily reduce the environmental impact of the AM process in the pre-production and production stages until AM technology is developed to reduce energy consumption [274,276,277].

Additive technology has the potential to contribute to sustainable development in many areas through innovation, waste reduction, and the optimization of manufacturing processes. However, while it offers many potential sustainability benefits, there are still a number of challenges that could impact its development and effectiveness. Some of the key challenges that could impact the development of additive technology in the context of sustainability are as follows:

1. Many current 3D printing materials are based on plastics, which can cause pollution and are difficult to recycle. There is an urgent need to develop more sustainable materials, such as those that are biodegradable or based on renewable resources. Recycling processes for these materials must be made more efficient and widely available to minimize their negative impact on the environment.
2. The generation of excessive waste and energy consumption during the 3D printing process can be detrimental to sustainability. Research into new methods and technologies that minimize waste and energy consumption is essential.
3. Future research should focus on improving the sustainability of AM technology by developing lower-energy powder manufacturing technologies, analyzing the impact of key parameters (such as specific energy consumption, build rate, powder yield, etc.) on the life cycle assessment of the AM process, optimizing key parameters for an efficient result, and increasing the production speed of the AM process. This will also improve the economics of the AM process by reducing the cost of producing the required parts [277].
4. As 3D printing grows in popularity, there is a need to ensure the scalability of manufacturing processes and the availability of suitable raw materials. It is important to ensure that raw materials are ethical, sustainable and do not lead to the depletion of natural resources.
5. The use of 3D printing in some sectors, such as medicine or aerospace, may require compliance with strict safety standards and norms, posing a challenge for the technology.
6. Many people, both consumers and businesses, may not be aware of the potential benefits and challenges of 3D printing in the context of sustainability. Education and awareness are key to the sustainable adoption of 3D printing technology.
7. The lack of consistent standards and regulations for 3D printing can make it difficult to control the technology's environmental impact. Establishing consistent standards for sustainable 3D printing is essential. Developing 3D printing with these challenges in mind can help to create more sustainable and environmentally friendly practices in the manufacturing industry. Separately, research into additive manufacturing applied to process/chemical engineering is a rapidly growing field. As technology advances and environmental awareness increases, it is expected that these challenges will be addressed and contribute to the further development of sustainable solutions in the field of 3D printing.

4. Conclusions

Three-dimensional printing can be a significant factor in optimizing heat transfer in a variety of applications, while contributing to sustainability. Incremental technology enables the creation of complex cooling structures and the production of coolers with custom shapes and sizes tailored to specific application needs that are difficult to achieve using traditional manufacturing methods. As a result, heat transfer performance can be optimized while minimizing material consumption, achieving very high compactness, in the order of 700 to even 5000 m²/m³.

Incremental technology enables the design of lightweight structures and the use of advanced high-thermal-conductivity materials (an example is the printing of MM-AM and the production of composites with increased conductivity of up to approximately

300%) adapted to the 3D printing process, which is particularly important in industries where weight is an issue (such as aerospace, e.g., an aerospace bracket with greater rigidity than its conventionally manufactured counterpart, while weighing 15% less). This helps to reduce energy and material consumption. Three-dimensional printing makes it possible to produce complex structures and designs without traditional material processing, minimizing waste. These processes can be more sustainable if raw materials are selected and processed according to sustainable principles. In the electronics sector, 3D printing can support the development of more efficient cooling systems, which is important for increasing the performance of electronic devices (15–65% increase in heat transfer compared to conventional heat exchangers). At the same time, it enables the production of custom heat exchangers tailored to specific applications. This increases the efficiency of heat exchange and minimizes energy loss. In the construction industry, 3D printing can be used to create smart structures that optimize heat exchange within buildings, improving energy efficiency. Currently, the main applications include prototyping, proof of concept, research/education/research and development, manufacturing, and the production of spare parts, more or less evenly distributed across various industries such as aerospace, technology, consumer goods, automotive, industrial goods, medical, and education. It is also clear that multidisciplinary and interdisciplinary collaboration, particularly between materials scientists, modelers, engineering practitioners, and 3D printing specialists, will be critical to delivering “next-generation” process engineering concepts.

Funding: This research received no external funding.

Data Availability Statement: Not applicable.

Conflicts of Interest: The authors declare no conflict of interest.

Nomenclature

| | |
|------|--|
| AM | Additive manufacturing |
| CAD | Computer-aided design |
| CAM | Computer-aided manufacturing |
| CGDS | Cold gas dynamic spray |
| DMLS | Direct metal laser sintering |
| FDM | Fused deposition modeling |
| LCM | Lithography-based ceramic manufacturing |
| LIGA | Lithography, electroplating, and molding |
| LOM | Laminated object manufacturing |
| LPBF | Laser powder bed fusion |
| LPW | Laser polymer welding |
| SLM | Selective laser melting |
| SLS | Selective laser sintering |
| UAM | Ultrasonic additive manufacturing |
| SLA | Stereolithography |
| DIW | Direct inkjet writing |
| R2R | Roll-to-roll |
| IL | Imprint lithography |
| EFF | Extrusion free forming |
| DED | Directed energy deposition |

References

1. Tsangas, M.; Papamichael, I.; Zorpas, A.A. Sustainable Energy Planning in a New Situation. *Energies* **2023**, *16*, 1626. [[CrossRef](#)]
2. Tsangas, M.; Zorpas, A.A.; Jeguirim, M. Sustainable renewable energy policies and regulations, recent advances, and challenges. In *Renewable Energy Production and Distribution*; Elsevier: Amsterdam, The Netherlands, 2022; pp. 449–465. [[CrossRef](#)]
3. Gielen, D.; Boshell, F.; Saygin, D.; Bazilian, M.D.; Wagner, N.; Gorini, R. The role of renewable energy in the global energy transformation. *Energy Strategy Rev.* **2019**, *24*, 38–50. [[CrossRef](#)]
4. Atems, B.; Hotaling, C. The effect of renewable and nonrenewable electricity generation on economic growth. *Energy Policy* **2018**, *112*, 111–118. [[CrossRef](#)]

5. Muth, J.; Klunker, A.; Völlmecke, C. Putting 3D printing to good use—Additive Manufacturing and the Sustainable Development Goals. *Front. Sustain.* **2023**, *4*, 1196228. [[CrossRef](#)]
6. Shanmugam, V.; Das, O.; Neisiany, R.E.; Babu, K.; Singh, S.; Hedenqvist, M.S.; Berto, F.; Ramakrishna, S. Polymer Recycling in Additive Manufacturing: An Opportunity for the Circular Economy. *Mater. Circ. Econ.* **2020**, *2*, 11. [[CrossRef](#)]
7. Anwajler, B.; Zdybel, E.; Tomaszewska-Ciosk, E. Innovative Polymer Composites with Natural Fillers Produced by Additive Manufacturing (3D Printing)—A Literature Review. *Polymers* **2023**, *15*, 3534. [[CrossRef](#)] [[PubMed](#)]
8. Wang, Q.; Sun, J.; Yao, Q.; Ji, C.; Liu, J.; Zhu, Q. 3D printing with cellulose materials. *Cellulose* **2018**, *25*, 4275–4301. [[CrossRef](#)]
9. Sudamrao Getme, A.; Patel, B. A Review: Bio-fiber's as reinforcement in composites of polylactic acid (PLA). *Mater. Today Proc.* **2020**, *26*, 2116–2122. [[CrossRef](#)]
10. Arefin, A.M.E.; Khatri, N.R.; Kulkarni, N.; Egan, P.F. Polymer 3D Printing Review: Materials, Process, and Design Strategies for Medical Applications. *Polymers* **2021**, *13*, 1499. [[CrossRef](#)]
11. Chen, Z.; Li, Z.; Li, J.; Liu, C.; Lao, C.; Fu, Y.; Liu, C.; Li, Y.; Wang, P.; He, Y. 3D printing of ceramics: A review. *J. Eur. Ceram. Soc.* **2019**, *39*, 661–687. [[CrossRef](#)]
12. Buchanan, C.; Gardner, L. Metal 3D printing in construction: A review of methods, research, applications, opportunities and challenges. *Eng. Struct.* **2019**, *180*, 332–348. [[CrossRef](#)]
13. Nehme, S.; Abeidi, A. 3D concrete printing: Review. *Epitoanyag-J. Silic. Based Compos. Mater.* **2022**, *74*, 183–187. [[CrossRef](#)]
14. Fratello, V.S.; Rael, R. Innovating materials for large scale additive manufacturing: Salt, soil, cement and chardonnay. *Cem. Concr. Res.* **2020**, *134*, 106097. [[CrossRef](#)]
15. Richards, D.J.; Tan, Y.; Jia, J.; Yao, H.; Mei, Y. 3D Printing for Tissue Engineering. *Isr. J. Chem.* **2013**, *53*, 805–814. [[CrossRef](#)] [[PubMed](#)]
16. ISO/ASTM 52900:2021; Additive Manufacturing—General Principles—Fundamentals and Vocabulary. Principles for the Development of International Standards, Guides and Recommendations issued by the World Trade Organization Technical Barriers to Trade (TBT) Committee. ISO: Geneva, Switzerland, 2021.
17. Jafferson, J.M.; Sabareesh, M.C.; Sidharth, B.S. 3D printed fabrics using generative and material Driven design. *Mater. Today Proc.* **2021**, *46*, 1319–1327. [[CrossRef](#)]
18. Ryan, K.R.; Down, M.P.; Banks, C.E. Future of additive manufacturing: Overview of 4D and 3D printed smart and advanced materials and their applications. *Chem. Eng. J.* **2021**, *403*, 126162. [[CrossRef](#)]
19. King, D.L.; Babasola, A.; Rozario, J.; Pearce, J.M. Mobile Open-Source Solar-Powered 3-D Printers for Distributed Manufacturing in Off-Grid Communities. *Chall. Sustain.* **2014**, *2*, 18–27. [[CrossRef](#)]
20. Ford, S.; Minshall, T. Invited review article: Where and how 3D printing is used in teaching and education. *Addit. Manuf.* **2019**, *25*, 131–150. [[CrossRef](#)]
21. Gebler, M.; Schoot Uiterkamp, A.J.M.; Visser, C. A global sustainability perspective on 3D printing technologies. *Energy Policy* **2014**, *74*, 158–167. [[CrossRef](#)]
22. Olsson, A.; Hellsing, M.S.; Rennie, A.R. New possibilities using additive manufacturing with materials that are difficult to process and with complex structures. *Phys. Scr.* **2017**, *92*, 053002. [[CrossRef](#)]
23. Li, C.; Pisignano, D.; Zhao, Y.; Xue, J. Advances in Medical Applications of Additive Manufacturing. *Engineering* **2020**, *6*, 1222–1231. [[CrossRef](#)]
24. Attaran, M. The rise of 3-D printing: The advantages of additive manufacturing over traditional manufacturing. *Bus. Horiz.* **2017**, *60*, 677–688. [[CrossRef](#)]
25. Srinivasan, R.; Giannikas, V.; McFarlane, D.; Thorne, A. Customising with 3D printing: The role of intelligent control. *Comput. Ind.* **2018**, *103*, 38–46. [[CrossRef](#)]
26. Ford, S.; Despeisse, M. Additive manufacturing and sustainability: An exploratory study of the advantages and challenges. *J. Clean. Prod.* **2016**, *137*, 1573–1587. [[CrossRef](#)]
27. Hopkinson, N.; Hague, R.J.M.; Dickens, P.M. (Eds.) *Rapid Manufacturing*; Wiley: New York, NY, USA, 2005. [[CrossRef](#)]
28. Zhang, Y.; Qin, B.; Chan, K.; Lupoi, R.; Yin, S.; Xie, Y.; Ye, S.; Yu, P.; Ke, H.; Wang, W. Enhancement on mechanical properties of CoCrNi medium entropy alloy via cold spray additive manufacturing associated with sintering. *J. Manuf. Process.* **2023**, *94*, 413–423. [[CrossRef](#)]
29. Zou, B.; Wang, L.; Zhang, Y.; Liu, Y.; Ouyang, Q.; Jin, S.; Zhang, D.; Yan, W.; Li, Z. Enhanced strength and ductility of metal composites with intragranularly dispersed reinforcements by additive manufacturing. *Mater. Res. Lett.* **2023**, *11*, 360–366. [[CrossRef](#)]
30. Zheng, X.; Williams, C.; Spadaccini, C.M.; Shea, K. Perspectives on multi-material additive manufacturing. *J. Mater. Res.* **2021**, *36*, 3549–3557. [[CrossRef](#)]
31. Zhang, R.; Jiang, F.; Xue, L.; Yu, J. Review of Additive Manufacturing Techniques for Large-Scale Metal Functionally Graded Materials. *Crystals* **2022**, *12*, 858. [[CrossRef](#)]
32. Wang, F.; Liu, C.; Yang, H.; Wang, H.; Zhang, H.; Zeng, X.; Wang, C.; Zhang, W.; Lv, W.; Zhu, P.; et al. 4D printing of ceramic structures. *Addit. Manuf.* **2023**, *63*, 103411. [[CrossRef](#)]
33. Pearce, J.M.; Blair, C.M.; Laciak, K.J.; Andrews, R.; Nosrat, A.; Zelenika-Zovko, I. 3-D Printing of Open Source Appropriate Technologies for Self-Directed Sustainable Development. *J. Sustain. Dev.* **2010**, *3*, 17–21. [[CrossRef](#)]

34. McDonough, J.R. A perspective on the current and future roles of additive manufacturing in process engineering, with an emphasis on heat transfer. *Therm. Sci. Eng. Prog.* **2020**, *19*, 100594. [CrossRef]
35. Decker, N.; Lyu, M.; Wang, Y.; Huang, Q. Geometric Accuracy Prediction and Improvement for Additive Manufacturing Using Triangular Mesh Shape Data. *J. Manuf. Sci. Eng.* **2021**, *143*, 6. [CrossRef]
36. Huang, Q.; Zhang, J.; Sabbaghi, A.; Dasgupta, T. Optimal offline compensation of shape shrinkage for three-dimensional printing processes. *IIE Trans.* **2015**, *47*, 431–441. [CrossRef]
37. Bacciaglia, A.; Ceruti, A. Efficient toolpath planning for collaborative material extrusion machines. *Rapid Prototyp. J.* **2023**, *29*, 1814–1828. [CrossRef]
38. Fontaine, N. Modular User-Configurable Multi-Part 3D Layering System and Hot End Assembly. U.S. Patent 14/845,803, 4 September 2015.
39. Frutuoso, N.A.M.d.M. Tool path generation for hybrid additive manufacturing. In Proceedings of the Solid Freeform Fabrication Symposium—An Additive Manufacturing, Austin, TX, USA, 13–15 August 2018.
40. Leite, M.; Frutuoso, N.; Soares, B.; Ventura, R. Multiple collaborative printing heads in fdm: The issues in process. In Proceedings of the 29th Annual International Solid Freeform Fabrication Symposium, Austin, TX, USA, 13–15 August 2018.
41. Leite, M. 3D printing of large parts using multiple collaborative deposition heads—A case study with FDM. In Proceedings of the 3rd International Conference on Progress in Additive Manufacturing, Singapore, 14–17 May 2018.
42. Zhang, X. Large-scale 3D printing by a team of mobile robots. *Autom. Constr.* **2018**, *95*, 98–106. [CrossRef]
43. McPherson, J.; Zhou, W. A chunk-based slicer for cooperative 3D printing. *Rapid Prototyp. J.* **2018**, *24*, 1436–1446. [CrossRef]
44. Afsharkohan, M.S.; Dehrooyeh, S.; Sohrabian, M.; Vaseghi, M. Influence of processing parameters tuning and rheological characterization on improvement of mechanical properties and fabrication accuracy of 3D printed models. *Rapid Prototyp. J.* **2023**, *29*, 867–881. [CrossRef]
45. Kaur, I.; Singh, P. State-of-the-art in heat exchanger additive manufacturing. *Int. J. Heat Mass Transf.* **2021**, *178*, 121600. [CrossRef]
46. Liu, P.S.; Chen, G.F. *Porous Materials*; Elsevier: Amsterdam, The Netherlands, 2014. [CrossRef]
47. Ashby, M.F. The properties of foams and lattices. *Philos. Trans. R. Soc. A Math. Phys. Eng. Sci.* **2006**, *364*, 15–30. [CrossRef]
48. Kaur, I.; Singh, P. Critical evaluation of additively manufactured metal lattices for viability in advanced heat exchangers. *Int. J. Heat Mass Transf.* **2021**, *168*, 120858. [CrossRef]
49. Liu, F. Laser-Induced Graphene Enabled Additive Manufacturing of Multifunctional 3D Architectures with Freeform Structures. *Adv. Sci.* **2023**, *10*, 4. [CrossRef]
50. Du Plessis, A.; Broeckhoven, C.; Yadroitsava, I.; Yadroitsev, I.; Hands, C.H.; Kunju, R.; Bhate, D. Beautiful and Functional: A Review of Biomimetic Design in Additive Manufacturing. *Addit. Manuf.* **2019**, *27*, 408–427. [CrossRef]
51. Dutkowski, K.; Kruzal, M.; Rokosz, K. Review of the State-of-the-Art Uses of Minimal Surfaces in Heat Transfer. *Energies* **2022**, *15*, 7994. [CrossRef]
52. Vignoles, G.L.; Rochais, D.; Chupin, S. Computation of the conducto-radiative effective heat conductivity of porous media defined by Triply Periodic Minimal Surfaces. *Int. J. Therm. Sci.* **2021**, *159*, 106598. [CrossRef]
53. Fan, Z.; Gao, R.; Liu, S. A novel battery thermal management system based on P type triply periodic minimal surface. *Int. J. Heat Mass Transf.* **2022**, *194*, 123090. [CrossRef]
54. Chen, L.Y.; Liang, S.X.; Liu, Y.; Zhang, L.C. Additive manufacturing of metallic lattice structures: Unconstrained design, accurate fabrication, fascinated performances, and challenges. *Mater. Sci. Eng. R Rep.* **2021**, *146*, 100648. [CrossRef]
55. Genç, A.M.; Vatanserver, C.; Koçak, M.; Karadeniz, Z.H. Investigation of additively manufactured triply periodic minimal surfaces as an air-to-air heat exchanger. In Proceedings of the CLIMA 2022 The 14th REHVA HVAC World Congress, Rotterdam, The Netherlands, 22–25 May 2022.
56. Reynolds, B.W.; Fee, C.J.; Morison, K.R.; Holland, D.J. Characterisation of Heat Transfer within 3D Printed TPMS Heat Exchangers. *Int. J. Heat Mass Transf.* **2023**, *212*, 124264. [CrossRef]
57. Alteneji, M.; Ali, M.I.H.; Khan, K.A.; Al-Rub, R.K.A. Heat transfer effectiveness characteristics maps for additively manufactured TPMS compact heat exchangers. *Energy Storage Sav.* **2022**, *1*, 153–161. [CrossRef]
58. Cheng, Z.; Li, X.; Xu, R.; Jiang, P. Investigations on porous media customized by triply periodic minimal surface: Heat transfer correlations and strength performance. *Int. Commun. Heat Mass Transf.* **2021**, *129*, 105713. [CrossRef]
59. Khalil, M.; Hassan Ali, M.I.; Khan, K.A.; Abu Al-Rub, R. Forced convection heat transfer in heat sinks with topologies based on triply periodic minimal surfaces. *Case Stud. Therm. Eng.* **2022**, *38*, 102313. [CrossRef]
60. Raja, S.; Hamulczuk, D.; Dybeck Carlsson, S. Exploring a New Energy-Efficient Way to Heat Water Design of a Heat Exchanger for Laundry Machine Applications Produced Using Additive Manufacturing. Available online: <https://odr.chalmers.se/handle/20.500.12380/302189?mode=full> (accessed on 10 May 2024).
61. Dixit, T.; Al-Hajri, E.; Paul, M.C.; Nithiarasu, P.; Kumar, S. High performance, microarchitected, compact heat exchanger enabled by 3D printing. *Appl. Therm. Eng.* **2022**, *210*, 118339. [CrossRef]
62. Yun, S.; Kwon, J.; Lee, D.; Shin, H.H.; Kim, Y. Heat transfer and stress characteristics of additive manufactured FCCZ lattice channel using thermal fluid-structure interaction model. *Int. J. Heat Mass Transf.* **2020**, *149*, 119187. [CrossRef]
63. Plant, R.D.; Saghri, M.Z. Numerical and experimental investigation of high concentration aqueous alumina nanofluids in a two and three channel heat exchanger. *Int. J. Thermofluids* **2021**, *9*, 100055. [CrossRef]

64. Thompson, S.M.; Aspin, Z.S.; Shamsaei, N.; Elwany, A.; Bian, L. Additive manufacturing of heat exchangers: A case study on a multi-layered Ti–6Al–4V oscillating heat pipe. *Addit. Manuf.* **2015**, *8*, 163–174. [[CrossRef](#)]
65. Iasiello, M.; Cunsolo, S.; Bianco, N.; Chiu, W.K.S.; Naso, V. Developing thermal flow in open-cell foams. *Int. J. Therm. Sci.* **2017**, *111*, 129–137. [[CrossRef](#)]
66. Pelanconi, M.; Zavattoni, S.; Cornolti, L.; Puragliesi, R.; Arrivabeni, E.; Ferrari, L.; Gianella, S.; Barbato, M.; Ortona, A. Application of Ceramic Lattice Structures to Design Compact, High Temperature Heat Exchangers: Material and Architecture Selection. *Materials* **2021**, *14*, 3225. [[CrossRef](#)] [[PubMed](#)]
67. Aider, Y.; Kaur, I.; Cho, H.; Singh, P. Periodic heat transfer characteristics of additively manufactured lattices. *Int. J. Heat Mass Transf.* **2022**, *189*, 122692. [[CrossRef](#)]
68. Butler, C.; Babu, S.; Lundy, R.; Meehan, R.R.; Punch, J.; Jeffers, N. Effects of processing parameters and heat treatment on thermal conductivity of additively manufactured AlSi10Mg by selective laser melting. *Mater. Charact.* **2021**, *173*, 110945. [[CrossRef](#)]
69. Lorenzon, A.; Vaglio, E.; Casarsa, L.; Sortino, M.; Totis, G.; Saragò, G.; Lendormy, E.; Raukola, J. Heat transfer and pressure loss performances for additively manufactured pin fin arrays in annular channels. *Appl. Therm. Eng.* **2022**, *202*, 117851. [[CrossRef](#)]
70. Anvari, A.; Azimi Yancheshme, A.; Kekre, K.M.; Ronen, A. State-of-the-art methods for overcoming temperature polarization in membrane distillation process: A review. *J. Membr. Sci.* **2020**, *616*, 118413. [[CrossRef](#)]
71. Mousa, M.H.; Miljkovic, N.; Nawaz, K. Review of heat transfer enhancement techniques for single phase flows. *Renew. Sustain. Energy Rev.* **2021**, *137*, 110566. [[CrossRef](#)]
72. Shahbazi, A.; Ashtiani, H.A.D.; Afshar, H.; Jafarkazemi, F. Optimization of the SMX static mixer types thermal and hydraulic performance by coupling CFD-Genetic Algorithm. *Int. Commun. Heat Mass Transf.* **2021**, *126*, 105388. [[CrossRef](#)]
73. Sélo, R.R.J.; Catchpole-Smith, S.; Maskery, I.; Ashcroft, I.; Tuck, C. On the thermal conductivity of AlSi10Mg and lattice structures made by laser powder bed fusion. *Addit. Manuf.* **2020**, *34*, 101214. [[CrossRef](#)]
74. Tiwari, R.; Andhare, R.S.; Shooshtari, A.; Ohadi, M. Development of an additive manufacturing-enabled compact manifold microchannel heat exchanger. *Appl. Therm. Eng.* **2019**, *147*, 781–788. [[CrossRef](#)]
75. Jha, V.; Dessiatoun, S.; Shooshtari, A.; Al-hajri, E.S.; Ohadi, M.M. Experimental Characterization of a Nickel Alloy-Based Manifold-Microgroove Evaporator. *Heat Transf. Eng.* **2015**, *36*, 33–42. [[CrossRef](#)]
76. Andhare, R.S.; Shooshtari, A.; Dessiatoun, S.V.; Ohadi, M.M. Heat transfer and pressure drop characteristics of a flat plate manifold microchannel heat exchanger in counter flow configuration. *Appl. Therm. Eng.* **2016**, *96*, 178–189. [[CrossRef](#)]
77. Arie, M.A.; Shooshtari, A.H.; Dessiatoun, S.V.; Ohadi, M.M. *Performance Characterization of an Additively Manufactured Titanium (Ti64) Heat Exchanger for an Air-Water Cooling Application*; American Society of Mechanical Engineers: New York, NY, USA, 2016.
78. Ho, J.Y.; Leong, K.C.; Wong, T.N. Experimental and numerical investigation of forced convection heat transfer in porous lattice structures produced by selective laser melting. *Int. J. Therm. Sci.* **2019**, *137*, 276–287. [[CrossRef](#)]
79. Ho, J.Y.; Leong, K.C. Cylindrical porous inserts for enhancing the thermal and hydraulic performance of water-cooled cold plates. *Appl. Therm. Eng.* **2017**, *121*, 863–878. [[CrossRef](#)]
80. Broughton, J.; Joshi, Y.K. Comparison of Single-Phase Convection in Additive Manufactured Versus Traditional Metal Foams. *J. Heat Transf.* **2020**, *142*, 8. [[CrossRef](#)]
81. Zhai, Y.L.; Xia, G.D.; Liu, X.F.; Wang, J. Characteristics of entropy generation and heat transfer in double-layered micro heat sinks with complex structure. *Energy Convers. Manag.* **2015**, *103*, 477–486. [[CrossRef](#)]
82. Dhaiban, H.T.; Hussein, M.A. The Optimal Design of Heat Sinks: A Review. *J. Appl. Comput. Mech.* **2020**, *64*, 1030–1043.
83. Gradla, P.; Cervoneb, A.; Colonna, P. Integral Channel Nozzles and Heat Exchangers using Additive Manufacturing Directed Energy Deposition NASA HR-1 Alloy. In Proceedings of the 73rd International Astronautical Congress, Paris, France, 18–22 September 2022; pp. 1–14.
84. Blakey-Milner, B.; Gradl, P.; Snedden, G.; Brooks, M.; Pitot, J.; Lopez, E.; Leary, M.; Berto, F.; Du Plessis, A. Metal additive manufacturing in aerospace: A review. *Mater. Des.* **2021**, *209*, 110008. [[CrossRef](#)]
85. Yeranee, K.; Rao, Y.; Xu, C.; Zhang, Y.; Su, X. Turbulent Flow Heat Transfer and Thermal Stress Improvement of Gas Turbine Blade Trailing Edge Cooling with Diamond-Type TPMS Structure. *Aerospace* **2023**, *11*, 37. [[CrossRef](#)]
86. Poole, S.; Phillips, R. Rapid prototyping of small wind turbine blades using additive manufacturing. In Proceedings of the 2015 Pattern Recognition Association of South Africa and Robotics and Mechatronics International Conference (PRASA-RobMech), Port Elizabeth, South Africa, 26–27 November 2015; pp. 189–194. [[CrossRef](#)]
87. Rouway, M.; Nachtane, M.; Tarfaoui, M.; Chakhchaoui, N.; Omari, L.E.; Fraija, F.; Cherkaoui, O. 3D printing: Rapid manufacturing of a new small-scale tidal turbine blade. *Int. J. Adv. Manuf. Technol.* **2021**, *115*, 61–76. [[CrossRef](#)]
88. Sobes, V.; Hiscox, B.; Popov, E.; Archibald, R.; Hauck, C.; Betzler, B.; Terrani, K. AI-based design of a nuclear reactor core. *Sci. Rep.* **2021**, *11*, 19646. [[CrossRef](#)] [[PubMed](#)]
89. Shama, A.; Pouchon, M.A.; Clifford, I. Simulation of the microfluidic mixing and the droplet generation for 3D printing of nuclear fuels. *Addit. Manuf.* **2019**, *26*, 1–14. [[CrossRef](#)]
90. Papadimitriou, I.; Just, M. Manufacturing of Structural Components for Internal Combustion Engine, Electric Motor and Battery Using Casting and 3D Printing. In *Advances in Engine and Powertrain Research and Technology. Mechanisms and Machine Science*; Springer: Cham, Switzerland, 2022; pp. 383–418. [[CrossRef](#)]
91. Koca, A.; Çalıřkan, C.İ.; Koç, E.; Akbal, Ö. A Novel 3D Printed Air-Cooled Fuel Cooler Heat Exchanger for Aviation Industry. *Heat Transf. Eng.* **2023**, *44*, 1350–1371. [[CrossRef](#)]

92. Wei, T.W.; Oprins, H.; Cherman, V.; Beyne, E.; Baelmans, M. Experimental and numerical investigation of direct liquid jet impinging cooling using 3D printed manifolds on lidded and lidless packages for 2.5D integrated systems. *Appl. Therm. Eng.* **2020**, *164*, 114535. [[CrossRef](#)]
93. Zaman, M.S.; Michalak, A.; Nasr, M.; da Silva, C.; Mills, J.K.; Amon, C.H.; Trescases, O. Multiphysics Optimization of Thermal Management Designs for Power Electronics Employing Impingement Cooling and Stereolithographic Printing. *IEEE Trans. Power Electron.* **2021**, *36*, 12769–12780. [[CrossRef](#)]
94. Haertel, J.H.K.; Nellis, G.F. A fully developed flow thermofluid model for topology optimization of 3D-printed air-cooled heat exchangers. *Appl. Therm. Eng.* **2017**, *119*, 10–24. [[CrossRef](#)]
95. Sabau, A.S.; Bejan, A.; Brownell, D.; Gluesenkamp, K.; Murphy, B.; List, I.I.F.; Carver, K.; Schaich, C.R.; Klett, J.W. Design, additive manufacturing, and performance of heat exchanger with a novel flow-path architecture. *Appl. Therm. Eng.* **2020**, *180*, 115775. [[CrossRef](#)]
96. Manaserh, Y.A.; Gharaibeh, A.R.; Tradat, M.I.; Rangarajan, S.; Sammakia, B.G.; Alissa, H.A. Multi-objective optimization of 3D printed liquid cooled heat sink with guide vanes for targeting hotspots in high heat flux electronics. *Int. J. Heat Mass Transf.* **2022**, *184*, 122287. [[CrossRef](#)]
97. Wits, W.W.; Jafari, D.; Jeggels, Y.; Van De Velde, S.; Jeggels, D.; Engelberts, N. Freeform-Optimized Shapes for Natural-Convection Cooling. In Proceedings of the 2018 24rd International Workshop on Thermal Investigations of ICs and Systems (THERMINIC), Stockholm, Sweden, 26–28 September 2018; pp. 1–6. [[CrossRef](#)]
98. Palumbo, J.; Tayyara, O.; Amon, C.H.; Chandra, S. Topologically optimized mini-channel heat sinks for reduced temperature non-uniformity. *Int. J. Heat Mass Transf.* **2023**, *214*, 124421. [[CrossRef](#)]
99. Degenstein, L.M.; Sameoto, D.; Hogan, J.D.; Asad, A.; Dolez, P.I. Smart Textiles for Visible and IR Camouflage Application: State-of-the-Art and Microfabrication Path Forward. *Micromachines* **2021**, *12*, 773. [[CrossRef](#)] [[PubMed](#)]
100. Mondal, K. Recent Advances in Soft E-Textiles. *Inventions* **2018**, *3*, 23. [[CrossRef](#)]
101. Chatterjee, K.; Ghosh, T.K. 3D Printing of Textiles: Potential Roadmap to Printing with Fibers. *Adv. Mater.* **2020**, *32*, 1902086. [[CrossRef](#)] [[PubMed](#)]
102. Katrycz, C.W.; Hatton, B.D. Bioinspired Microfluidic Cooling. In *Bioinspired Engineering of Thermal Materials*; Wiley: New York, NY, USA, 2018; pp. 129–158. [[CrossRef](#)]
103. Safdar, A.; He, H.Z.; Wei, L.; Snis, A.; Chavez de Paz, L.E. Effect of process parameters settings and thickness on surface roughness of EBM produced Ti-6Al-4V. *Rapid Prototyp. J.* **2012**, *18*, 401–408. [[CrossRef](#)]
104. Reis, N.C.; Vasco, J.C.; Barreiros, F.M. Conformal cooling by SLM to improve injection moulding. In Proceedings of the Polymers and Moulds Innovations, Guimarães, Portugal, 19–21 September 2018.
105. Brandner, J.J.; Hansjosten, E.; Anurjew, E.; Pflöging, W.; Schubert, K. Microstructure devices generation by selective laser melting. In *Proceedings Volume 6459, Laser-Based Micro- and Nanopackaging and Assembly*; 645911; Pflöging, W., Lu, Y., Washio, K., Bachmann, F.G., Hoving, W., Eds.; SPIE: Bellingham, WA, USA, 2007. [[CrossRef](#)]
106. Wei, X.; Li, D.; Jiang, W.; Gu, Z.; Wang, X.; Zhang, Z.; Sun, Z. 3D Printable Graphene Composite. *Sci. Rep.* **2015**, *5*, 11181. [[CrossRef](#)] [[PubMed](#)]
107. Wang, J.; Liu, Y.; Fan, Z.; Wang, W.; Wang, B.; Guo, Z. Ink-based 3D printing technologies for graphene-based materials: A review. *Adv. Compos. Hybrid Mater.* **2019**, *2*, 1–33. [[CrossRef](#)]
108. Guo, H.; Lv, R.; Bai, S. Recent advances on 3D printing graphene-based composites. *Nano Mater. Sci.* **2019**, *1*, 101–115. [[CrossRef](#)]
109. Rinaldi, M.; Ferrara, M.; Pigliaru, L.; Allegranza, C.; Nanni, F. Additive manufacturing of polyether ether ketone-based composites for space application: A mini-review. *CEAS Space J.* **2023**, *15*, 77–87. [[CrossRef](#)]
110. Ritter, T.; McNiffe, E.; Higgins, T.; Sam-Daliri, O.; Flanagan, T.; Walls, M.; Ghabezi, P.; Finnegan, W.; Mitchell, S.; Harrison, N.M. Design and Modification of a Material Extrusion 3D Printer to Manufacture Functional Gradient PEEK Components. *Polymers* **2023**, *15*, 3825. [[CrossRef](#)] [[PubMed](#)]
111. Jayaraghu, T.K.; Karthik, K.; Yaswanth, A.; Venkatesan, M. Nozzle flow characteristics of P.E.E.K (Poly-ether ether ketone) material used in 3D-printing. *Mater Today Proc.* **2021**, *44*, 2963–2967. [[CrossRef](#)]
112. Chen, H.; Wang, K.; Chen, Y.; Le, H. Mechanical and Thermal Properties of Multilayer-Coated 3D-Printed Carbon Fiber Reinforced Nylon Composites. *J. Compos. Sci.* **2023**, *7*, 297. [[CrossRef](#)]
113. Wojtyła, S.; Klama, P.; Baran, T. Is 3D printing safe? Analysis of the thermal treatment of thermoplastics: ABS, PLA, PET, and nylon. *J. Occup. Environ. Hyg.* **2017**, *14*, D80–D85. [[CrossRef](#)] [[PubMed](#)]
114. Guessasma, S.; Belhabib, S.; Nouri, H. Effect of printing temperature on microstructure, thermal behavior and tensile properties of 3D printed nylon using fused deposition modeling. *J. Appl. Polym. Sci.* **2021**, *138*, 50162. [[CrossRef](#)]
115. Reizabal, A.; Devlin, B.L.; Paxton, N.C.; Saiz, P.G.; Liashenko, I.; Luposchinsky, S.; Woodruff, M.A.; Lanceros-Mendez, S.; Dalton, P.D. Melt Electrowriting of Nylon-12 Microfibers with an Open-Source 3D Printer. *Macromol. Rapid Commun.* **2023**, *44*, 2300424. [[CrossRef](#)] [[PubMed](#)]
116. Tsopanos, S.; Sutcliffe, C.J.; Owen, I. The manufacture of micro cross-flow heat exchangers by selective laser melting. In Proceedings of the 5th Internal Conference on Enhanced, Compact and Ultra-Compact Heat Exchangers: Science, Engineering and Technology, Hoboken, NJ, USA, 11–16 September 2005.
117. Lind, A.; Vistad, Ø.; Sunding, M.F.; Andreassen, K.A.; Cavka, J.H.; Grande, C.A. Multi-purpose structured catalysts designed and manufactured by 3D printing. *Mater. Des.* **2020**, *187*, 108377. [[CrossRef](#)]

118. Dreier, T.; Riaz, A.; Ahrend, A.; Polley, C.; Bode, S.; Milkereit, B.; Seitz, H. 3D printing of aluminum oxide via composite extrusion modeling using a ceramic injection molding feedstock. *Mater. Des.* **2023**, *227*, 111806. [[CrossRef](#)]
119. Yang, D.; Zhang, H.; Wu, J.; McCarthy, E.D. Fibre flow and void formation in 3D printing of short-fibre reinforced thermoplastic composites: An experimental benchmark exercise. *Addit. Manuf.* **2021**, *37*, 101686. [[CrossRef](#)]
120. Nakagawa, Y.; Mori, K.; Yoshino, M. Laser-assisted 3D printing of carbon fibre reinforced plastic parts. *J. Manuf. Processes* **2022**, *73*, 375–384. [[CrossRef](#)]
121. Ibrahim, Y.; Elkholy, A.; Schofield, J.S.; Melenka, G.W.; Kempers, R. Effective thermal conductivity of 3D-printed continuous fiber polymer composites. *Adv. Manuf. Polym. Compos. Sci.* **2020**, *6*, 17–28. [[CrossRef](#)]
122. Ji, J.; Chiang, S.W.; Liu, M.; Liang, X.; Li, J.; Gan, L.; He, Y.; Li, B.; Kang, F.; Du, H. Enhanced thermal conductivity of alumina and carbon fibre filled composites by 3-D printing. *Thermochim. Acta* **2020**, *690*, 178649. [[CrossRef](#)]
123. Laureto, J.; Tomasi, J.; King, J.A.; Pearce, J.M. Thermal properties of 3-D printed polylactic acid-metal composites. *Prog. Addit. Manuf.* **2017**, *2*, 57–71. [[CrossRef](#)]
124. Kailkhura, G.; Mandel, R.K.; Shooshtari, A.; Ohadi, M. Numerical and Experimental Study of a Novel Additively Manufactured Metal-Polymer Composite Heat-Exchanger for Liquid Cooling Electronics. *Energies* **2022**, *15*, 598. [[CrossRef](#)]
125. Ibrahim, Y.; Kempers, R. Effective thermal conductivity of 3D-printed continuous wire polymer composites. *Prog. Addit. Manuf.* **2022**, *7*, 699–712. [[CrossRef](#)]
126. Deisenroth, D.C.; Moradi, R.; Shooshtari, A.H.; Singer, F.; Bar-Cohen, A.; Ohadi, M. Review of Heat Exchangers Enabled by Polymer and Polymer Composite Additive Manufacturing. *Heat Transf. Eng.* **2018**, *39*, 1648–1664. [[CrossRef](#)]
127. Bandyopadhyay, A.; Heer, B. Additive manufacturing of multi-material structures. *Mater. Sci. Eng. R Rep.* **2018**, *129*, 1–16. [[CrossRef](#)]
128. Yap, C.Y. Review of selective laser melting: Materials and applications. *Appl. Phys. Rev.* **2015**, *2*, 4. [[CrossRef](#)]
129. Onuikwe, B.; Heer, B.; Bandyopadhyay, A. Additive manufacturing of Inconel 718—Copper alloy bimetallic structure using laser engineered net shaping (LENSTM). *Addit. Manuf.* **2018**, *21*, 133–140.
130. Heer, B.; Bandyopadhyay, A. Compositionally graded magnetic-nonmagnetic bimetallic structure using laser engineered net shaping. *Mater. Lett.* **2018**, *216*, 16–19. [[CrossRef](#)]
131. Scheithauer, U. Potentials and Challenges of Additive Manufacturing Technologies for Heat Exchanger. In *Advances in Heat Exchangers*; IntechOpen: London, UK, 2019.
132. Kamal, M.; Rizza, G. Design for metal additive manufacturing for aerospace applications. In *Additive Manufacturing for the Aerospace Industry*; Elsevier: Amsterdam, The Netherlands, 2019; pp. 67–86.
133. Bacellar, D.; Aute, V.; Huang, Z.; Radermacher, R. Design optimization and validation of high-performance heat exchangers using approximation assisted optimization and additive manufacturing. *Sci. Technol. Built Environ.* **2017**, *23*, 896–911. [[CrossRef](#)]
134. Alshare, A.A.; Calzone, F.; Muzzupappa, M. Hydraulic manifold design via additive manufacturing optimized with CFD and fluid-structure interaction simulations. *Rapid Prototyp. J.* **2019**, *25*, 1516–1524. [[CrossRef](#)]
135. Gutmann, B. Design and 3D printing of a stainless steel reactor for continuous difluoromethylations using fluoroform. *React. Chem. Eng.* **2017**, *2*, 919–927. [[CrossRef](#)]
136. McGlen, R.J. An introduction to additive manufactured heat pipe technology and advanced thermal management products. *Therm. Sci. Eng. Prog.* **2021**, *25*, 100941. [[CrossRef](#)]
137. Kong, D.; Zhang, Y.; Liu, S. Convective heat transfer enhancement by novel honeycomb-core in sandwich panel exchanger fabricated by additive manufacturing. *Appl. Therm. Eng.* **2019**, *163*, 114408. [[CrossRef](#)]
138. Da Silva, R.P.; Morteau, M.V.; de Paiva, K.V.; Beckedorff, L.E.; Oliveira, J.L.; Brandão, F.G.; Monteiro, A.S.; Carvalho, C.S.; Oliveira, H.R.; Borges, D.G.; et al. Thermal and hydrodynamic analysis of a compact heat exchanger produced by additive manufacturing. *Appl. Therm. Eng.* **2021**, *193*, 116973. [[CrossRef](#)]
139. Scheithauer, U.; Schwarzer, E.; Moritz, T.; Michaelis, A. Additive Manufacturing of Ceramic Heat Exchanger: Opportunities and Limits of the Lithography-Based Ceramic Manufacturing (LCM). *J. Mater. Eng. Perform.* **2018**, *27*, 14–20. [[CrossRef](#)]
140. Pelanconi, M.; Barbato, M.; Zavattoni, S.; Vignoles, G.L.; Ortona, A. Thermal design, optimization and additive manufacturing of ceramic regular structures to maximize the radiative heat transfer. *Mater. Des.* **2019**, *163*, 107539. [[CrossRef](#)]
141. Niknam, S.A.; Mortazavi, M.; Li, D. Additively manufactured heat exchangers: A review on opportunities and challenges. *Int. J. Adv. Manuf. Technol.* **2021**, *112*, 601–618. [[CrossRef](#)]
142. Careri, F.; Khan, R.H.U.; Todd, C.; Attallah, M.M. Additive manufacturing of heat exchangers in aerospace applications: A review. *Appl. Therm. Eng.* **2023**, *235*, 121387. [[CrossRef](#)]
143. Gulia, V.; Sur, A. A comprehensive review on microchannel heat exchangers, heat sink, and polymer heat exchangers: Current state of the art. *Front. Heat Mass Transf.* **2022**, *18*, 1–10. [[CrossRef](#)]
144. Kwon, B.; Liebenberg, L.; Jacobi, A.M.; King, W.P. Heat transfer enhancement of internal laminar flows using additively manufactured static mixers. *Int. J. Heat Mass Transf.* **2019**, *137*, 292–300. [[CrossRef](#)]
145. Kirsch, K.L.; Thole, K.A. Pressure loss and heat transfer performance for additively and conventionally manufactured pin fin arrays. *Int. J. Heat Mass Transf.* **2017**, *108*, 2502–2513. [[CrossRef](#)]
146. Du, L.; Hu, W. An overview of heat transfer enhancement methods in microchannel heat sinks. *Chem. Eng. Sci.* **2023**, *280*, 119081. [[CrossRef](#)]

147. Ventola, L.; Robotti, F.; Dialameh, M.; Calignano, F.; Manfredi, D.; Chiavazzo, E.; Asinari, P. Rough surfaces with enhanced heat transfer for electronics cooling by direct metal laser sintering. *Int. J. Heat Mass Transf.* **2014**, *75*, 58–74. [[CrossRef](#)]
148. Yu, H.; Li, T.; Zeng, X.; He, T.; Mao, N. A Critical Review on Geometric Improvements for Heat Transfer Augmentation of Microchannels. *Energies* **2022**, *15*, 9474. [[CrossRef](#)]
149. Huang, C.; Cai, W.; Wang, Y.; Liu, Y.; Li, Q.; Li, B. Review on the characteristics of flow and heat transfer in printed circuit heat exchangers. *Appl. Therm. Eng.* **2019**, *153*, 190–205. [[CrossRef](#)]
150. T'Joel, C.; Park, Y.; Wang, Q.; Sommers, A.; Han, X.; Jacobi, A. A review on polymer heat exchangers for HVAC&R applications. *Int. J. Refrig.* **2009**, *32*, 763–779.
151. Greiciunas, E.; Borman, D.; Summers, J.; Smith, S.J. Experimental and numerical study of the additive layer manufactured inter-layer channel heat exchanger. *Appl. Therm. Eng.* **2021**, *188*, 116501. [[CrossRef](#)]
152. Szymanski, P.; Mikielewicz, D. Additive Manufacturing as a Solution to Challenges Associated with Heat Pipe Production. *Materials* **2022**, *15*, 1609. [[CrossRef](#)]
153. Kappe, K.; Bihler, M.; Morawietz, K.; Hügenell, P.P.; Pfaff, A.; Hoschke, K. Design Concepts and Performance Characterization of Heat Pipe Wick Structures by LPBF Additive Manufacturing. *Materials* **2022**, *15*, 8930. [[CrossRef](#)] [[PubMed](#)]
154. Tsopanos, S.; Wong, M.; Owen, I.; Sutcliffe, C.J. Manufacturing novel heat transfer devices by selective laser melting. In *Manufacturing*; Begell House Inc.: Danbury, CT, USA, 2006. [[CrossRef](#)]
155. Wong, M.; Tsopanos, S.; Sutcliffe, C.J.; Owen, I. Selective laser melting of heat transfer devices. *Rapid Prototyp. J.* **2007**, *13*, 291–297. [[CrossRef](#)]
156. Wong, M.; Owen, I.; Sutcliffe, C.J. Pressure Loss and Heat Transfer Through Heat Sinks Produced by Selective Laser Melting. *Heat Transf. Eng.* **2009**, *30*, 1068–1076. [[CrossRef](#)]
157. Wong, M.; Owen, I.; Sutcliffe, C.J.; Puri, A. Convective heat transfer and pressure losses across novel heat sinks fabricated by Selective Laser Melting. *Int. J. Heat Mass Transf.* **2009**, *52*, 281–288. [[CrossRef](#)]
158. Pakkanen, J.; Calignano, F.; Trevisan, F.; Lorusso, M.; Ambrosio, E.P.; Manfredi, D.; Fino, P. Study of Internal Channel Surface Roughnesses Manufactured by Selective Laser Melting in Aluminum and Titanium Alloys. *Metall. Mater. Trans. A* **2016**, *47*, 3837–3844. [[CrossRef](#)]
159. Garde, K.; Davidson, J.; Mantell, S. *Design and Manufacturing of an Oil Cooler by Additive Manufacturing*; University of Minnesota: Minneapolis, MN, USA, 2017.
160. Korinko, P.S.; Bobbitt, J.; McKee, H.; List, F.; Carver, K. Characterization of Additively Manufactured Heat Exchanger Tubing. In *Volume 6A: Materials and Fabrication*; American Society of Mechanical Engineers: New York, NY, USA, 2017. [[CrossRef](#)]
161. Hathaway, B.J.; Garde, K.; Mantell, S.C.; Davidson, J.H. Design and characterization of an additive manufactured hydraulic oil cooler. *Int. J. Heat Mass Transf.* **2018**, *117*, 188–200. [[CrossRef](#)]
162. Yan, C.; Hao, L.; Hussein, A.; Bubb, S.L.; Young, P.; Raymont, D. Evaluation of light-weight AlSi10Mg periodic cellular lattice structures fabricated via direct metal laser sintering. *J. Mater. Process. Technol.* **2014**, *214*, 856–864. [[CrossRef](#)]
163. Arie, M.A.; Shooshtari, A.H.; Rao, V.V.; Dessiatoun, S.V.; Ohadi, M.M. Air-Side Heat Transfer Enhancement Utilizing Design Optimization and an Additive Manufacturing Technique. *J. Heat Transf.* **2017**, *139*, 031901. [[CrossRef](#)]
164. Stimpson, C.K.; Snyder, J.C.; Thole, K.A.; Mongillo, D. Roughness Effects on Flow and Heat Transfer for Additively Manufactured Channels. *J. Turbomach.* **2016**, *138*, 051008. [[CrossRef](#)]
165. Kirsch, K.L.; Thole, K.A. Heat Transfer and Pressure Loss Measurements in Additively Manufactured Wavy Microchannels. *J. Turbomach.* **2017**, *139*, 011007. [[CrossRef](#)]
166. Snyder, J.C.; Stimpson, C.K.; Thole, K.A.; Mongillo, D. Build Direction Effects on Additively Manufactured Channels. *J. Turbomach.* **2016**, *138*, 051006. [[CrossRef](#)]
167. Bernardin, J.D.; Ferguson, K.; Sattler, D.; Kim, S.-J. *The Design, Analysis, and Fabrication of an Additively Manufactured Twisted Tube Heat Exchanger*; American Society of Mechanical Engineers: New York, NY, USA, 2017. [[CrossRef](#)]
168. Gerstler, W.D.; Erno, D. Introduction of an additively manufactured multi-furcating heat exchanger. In Proceedings of the 2017 16th IEEE Intersociety Conference on Thermal and Thermomechanical Phenomena in Electronic Systems (ITherm), Orlando, FL, USA, 30 May–2 June 2017; pp. 624–633. [[CrossRef](#)]
169. Arie, M.A.; Shooshtari, A.H.; Ohadi, M.M. Experimental characterization of an additively manufactured heat exchanger for dry cooling of power plants. *Appl. Therm. Eng.* **2018**, *129*, 187–198. [[CrossRef](#)]
170. Ibrahim, O.T.; Monroe, J.G.; Thompson, S.M.; Shamsaei, N.; Bilheux, H.; Elwany, A.; Bian, L. An investigation of a multi-layered oscillating heat pipe additively manufactured from Ti-6Al-4V powder. *Int. J. Heat Mass Transf.* **2017**, *108*, 1036–1047. [[CrossRef](#)]
171. Jazi, H.R.S.; Mostaghimi, J.; Chandra, S.; Pershin, L.; Coyle, T. Spray-Formed, Metal-Foam Heat Exchangers for High Temperature Applications. *J. Therm. Sci. Eng. Appl.* **2009**, *1*, 031008. [[CrossRef](#)]
172. Cormier, Y.; Dupuis, P.; Jodoin, B.; Corbeil, A. Net Shape Fins for Compact Heat Exchanger Produced by Cold Spray. *J. Therm. Spray Technol.* **2013**, *22*, 1210–1221. [[CrossRef](#)]
173. Cormier, Y.; Dupuis, P.; Farjam, A.; Corbeil, A.; Jodoin, B. Additive manufacturing of pyramidal pin fins: Height and fin density effects under forced convection. *Int. J. Heat Mass Transf.* **2014**, *75*, 235–244. [[CrossRef](#)]
174. Dupuis, P.; Cormier, Y.; Farjam, A.; Jodoin, B.; Corbeil, A. Performance evaluation of near-net pyramidal shaped fin arrays manufactured by cold spray. *Int. J. Heat Mass Transf.* **2014**, *69*, 34–43. [[CrossRef](#)]

175. Farjam, A.; Cormier, Y.; Dupuis, P.; Jodoin, B.; Corbeil, A. Influence of Alumina Addition to Aluminum Fins for Compact Heat Exchangers Produced by Cold Spray Additive Manufacturing. *J. Therm. Spray Technol.* **2015**, *24*, 1256–1268. [[CrossRef](#)]
176. Cormier, Y.; Dupuis, P.; Jodoin, B.; Corbeil, A. Pyramidal Fin Arrays Performance Using Streamwise Anisotropic Materials by Cold Spray Additive Manufacturing. *J. Therm. Spray Technol.* **2016**, *25*, 170–182. [[CrossRef](#)]
177. Dupuis, P.; Cormier, Y.; Fenech, M.; Corbeil, A.; Jodoin, B. Flow structure identification and analysis in fin arrays produced by cold spray additive manufacturing. *Int. J. Heat Mass Transf.* **2016**, *93*, 301–313. [[CrossRef](#)]
178. Dupuis, P.; Cormier, Y.; Fenech, M.; Jodoin, B. Heat transfer and flow structure characterization for pin fins produced by cold spray additive manufacturing. *Int. J. Heat Mass Transf.* **2016**, *98*, 650–661. [[CrossRef](#)]
179. Harris, C.; Despa, M.; Kelly, K. Design and fabrication of a cross flow micro heat exchanger. *J. Microelectromech. Syst.* **2000**, *9*, 502–508. [[CrossRef](#)]
180. Arie, M.A.; Shooshtari, A.H.; Tiwari, R.; Dessiatoun, S.V.; Ohadi, M.M.; Pearce, J.M. Experimental characterization of heat transfer in an additively manufactured polymer heat exchanger. *Appl. Therm. Eng.* **2017**, *113*, 575–584. [[CrossRef](#)]
181. Rua, Y.; Muren, R.; Reckinger, S. Limitations of Additive Manufacturing on Microfluidic Heat Exchanger Components. *J. Manuf. Sci. Eng.* **2015**, *137*, 034504. [[CrossRef](#)]
182. Felber, R.A.; Nellis, G.; Rudolph, N. Design and Modeling of 3D-Printed Air-Cooled Heat Exchangers. In Proceedings of the International Refrigeration and Air Conditioning Conference, West Lafayette, IN, USA, 11–14 July 2016.
183. Cevallos, J.; Bar-Cohen, A.; Deisenroth, D.C. Thermal performance of a polymer composite webbed-tube heat exchanger. *Int. J. Heat Mass Transf.* **2016**, *98*, 845–856. [[CrossRef](#)]
184. Shulman, H.; Ross, N. *Additive Manufacturing for Cost Efficient Production of Compact Ceramic Heat Exchangers and Recuperators*; Ceralink Incorporated: Troy, NY, USA, 2015. [[CrossRef](#)]
185. Schwarzer, E.; Götz, M.; Markova, D.; Stafford, D.; Scheithauer, U.; Moritz, T. Lithography-based ceramic manufacturing (LCM)—Viscosity and cleaning as two quality influencing steps in the process chain of printing green parts. *J. Eur. Ceram. Soc.* **2017**, *37*, 5329–5338. [[CrossRef](#)]
186. Tarancón, A. 2022 roadmap on 3D printing for energy. *J. Phys. Energy* **2022**, *4*, 011501. [[CrossRef](#)]
187. Kim, F.; Kwon, B.; Eom, Y.; Lee, J.E.; Park, S.; Jo, S.; Park, S.H.; Kim, B.S.; Im, H.J.; Lee, M.H.; et al. 3D printing of shape-conformable thermoelectric materials using all-inorganic Bi₂Te₃-based inks. *Nat. Energy* **2018**, *3*, 301–309. [[CrossRef](#)]
188. Pesce, A.; Hornés, A.; Núñez, M.; Morata, A.; Torrell, M.; Tarancón, A. 3D printing the next generation of enhanced solid oxide fuel and electrolysis cells. *J. Mater. Chem. A Mater.* **2020**, *8*, 16926–16932. [[CrossRef](#)]
189. Trogadas, P.; Cho, J.I.; Neville, T.P.; Marquis, J.; Wu, B.; Brett, D.J.; Coppens, M.O. A lung-inspired approach to scalable and robust fuel cell design. *Energy Environ. Sci.* **2018**, *11*, 136–143. [[CrossRef](#)]
190. Breitwieser, M.; Klingele, M.; Vierrath, S.; Zengerle, R.; Thiele, S. Tailoring the Membrane-Electrode Interface in PEM Fuel Cells: A Review and Perspective on Novel Engineering Approaches. *Adv. Energy Mater.* **2018**, *8*, 1701257. [[CrossRef](#)]
191. Han, G.D.; Bae, K.; Kang, E.H.; Choi, H.J.; Shim, J.H. Inkjet Printing for Manufacturing Solid Oxide Fuel Cells. *ACS Energy Lett.* **2020**, *5*, 1586–1592. [[CrossRef](#)]
192. Sukeshini, M.A.; Cummins, R.; Reitz, T.L.; Miller, R.M. Ink-Jet Printing: A Versatile Method for Multilayer Solid Oxide Fuel Cells Fabrication. *J. Am. Ceram. Soc.* **2009**, *92*, 2913–2919. [[CrossRef](#)]
193. Klingele, M.; Breitwieser, M.; Zengerle, R.; Thiele, S. Direct deposition of proton exchange membranes enabling high performance hydrogen fuel cells. *J. Mater. Chem. A Mater.* **2015**, *3*, 11239–11245. [[CrossRef](#)]
194. Esposito, V.; Gadea, C.; Hjelm, J.; Marani, D.; Hu, Q.; Agersted, K.; Ramousse, S.; Jensen, S.H. Fabrication of thin yttria-stabilized-zirconia dense electrolyte layers by inkjet printing for high performing solid oxide fuel cells. *J. Power Sources* **2015**, *273*, 89–95. [[CrossRef](#)]
195. Hornés, A.; Pesce, A.; Hernández-Afonso, L.; Morata, A.; Torrell, M.; Tarancón, A. 3D Printing of Fuel Cells and Electrolyzers. In *3D Printing for Energy Applications*; Wiley: New York, NY, USA, 2021; pp. 273–306. [[CrossRef](#)]
196. Andersen, T.R.; Dam, H.F.; Hösel, M.; Helgesen, M.; Carlé, J.E.; Larsen-Olsen, T.T.; Gevorgyan, S.A.; Andreasen, J.W.; Adams, J.; Li, N.; et al. Scalable, ambient atmosphere roll-to-roll manufacture of encapsulated large area, flexible organic tandem solar cell modules. *Energy Environ. Sci.* **2014**, *7*, 2925. [[CrossRef](#)]
197. Knott, A.; Makarovskiy, O.; O’Shea, J.; Wu, Y.; Tuck, C. Scanning photocurrent microscopy of 3D printed light trapping structures in dye-sensitized solar cells. *Sol. Energy Mater. Sol. Cells* **2018**, *180*, 103–109. [[CrossRef](#)]
198. Van Dijk, L.; Marcus, E.A.P.; Oostra, A.J.; Schropp, R.E.I.; Di Vece, M. 3D-printed concentrator arrays for external light trapping on thin film solar cells. *Sol. Energy Mater. Sol. Cells* **2015**, *139*, 19–26. [[CrossRef](#)]
199. Huang, Q.Z.; Zhu, Y.Q.; Shi, J.F.; Wang, L.L.; Zhong, L.W.; Xu, G. Dye-sensitized solar cell module realized photovoltaic and photothermal highly efficient conversion via three-dimensional printing technology. *Chin. Phys. B* **2017**, *26*, 038401. [[CrossRef](#)]
200. Bernardi, M.; Ferralis, N.; Wan, J.H.; Villalon, R.; Grossman, J.C. Solar energy generation in three dimensions. *Energy Environ. Sci.* **2012**, *5*, 6880. [[CrossRef](#)]
201. Ahn, B.Y.; Lorang, D.J.; Duoss, E.B.; Lewis, J.A. Direct-write assembly of microperiodic planar and spanning ITO microelectrodes. *Chem. Commun.* **2010**, *46*, 7118. [[CrossRef](#)] [[PubMed](#)]
202. Mathies, F.; Eggers, H.; Richards, B.S.; Hernandez-Sosa, G.; Lemmer, U.; Paetzold, U.W. Inkjet-Printed Triple Cation Perovskite Solar Cells. *ACS Appl. Energy Mater.* **2018**, *1*, 1834–1839. [[CrossRef](#)]

203. Di Giacomo, F.; Fakharuddin, A.; Jose, R.; Brown, T.M. Progress, challenges and perspectives in flexible perovskite solar cells. *Energy Environ. Sci.* **2016**, *9*, 3007–3035. [[CrossRef](#)]
204. Wang, G.; Adil, M.A.; Zhang, J.; Wei, Z. Large-Area Organic Solar Cells: Material Requirements, Modular Designs, and Printing Methods. *Adv. Mater.* **2019**, *31*, 1805089. [[CrossRef](#)]
205. Jo, S.; Choo, S.; Kim, F.; Heo, S.H.; Son, J.S. Ink Processing for Thermoelectric Materials and Power-Generating Devices. *Adv. Mater.* **2019**, *31*, 1804930. [[CrossRef](#)] [[PubMed](#)]
206. He, M.; Zhao, Y.; Wang, B.; Xi, Q.; Zhou, J.; Liang, Z. 3D Printing Fabrication of Amorphous Thermoelectric Materials with Ultralow Thermal Conductivity. *Small* **2015**, *11*, 5889–5894. [[CrossRef](#)] [[PubMed](#)]
207. Oztan, C.; Ballikaya, S.; Ozgun, U.; Karkkainen, R.; Celik, E. Additive manufacturing of thermoelectric materials via fused filament fabrication. *Appl. Mater. Today* **2019**, *15*, 77–82. [[CrossRef](#)]
208. Qiu, J.; Yan, Y.; Luo, T.; Tang, K.; Yao, L.; Zhang, J.; Zhang, M.; Su, X.; Tan, G.; Xie, H.; et al. 3D Printing of highly textured bulk thermoelectric materials: Mechanically robust BiSbTe alloys with superior performance. *Energy Environ. Sci.* **2019**, *12*, 3106–3117. [[CrossRef](#)]
209. Shi, J.; Chen, H.; Jia, S.; Wang, W. 3D printing fabrication of porous bismuth antimony telluride and study of the thermoelectric properties. *J. Manuf. Processes* **2019**, *37*, 370–375. [[CrossRef](#)]
210. Saeidi-Javash, M.; Kuang, W.; Dun, C.; Zhang, Y. 3D Conformal Printing and Photonic Sintering of High-Performance Flexible Thermoelectric Films Using 2D Nanoplates. *Adv. Funct. Mater.* **2019**, *29*, 1901930. [[CrossRef](#)]
211. Burton, M.R.; Mehraban, S.; Beynon, D.; McGettrick, J.; Watson, T.; Lavery, N.P.; Carnie, M.J. 3D Printed SnSe Thermoelectric Generators with High Figure of Merit. *Adv. Energy Mater.* **2019**, *9*, 1900201. [[CrossRef](#)]
212. Eom, Y.; Kim, F.; Yang, S.E.; Son, J.S.; Chae, H.G. Rheological design of 3D printable all-inorganic inks using BiSbTe-based thermoelectric materials. *J. Rheol.* **2019**, *63*, 291–304. [[CrossRef](#)]
213. Dolzhnikov, D.S.; Zhang, H.; Jang, J.; Son, J.S.; Panthani, M.G.; Shibata, T.; Chattopadhyay, S.; Talapin, D.V. Composition-matched molecular “solders” for semiconductors. *Science* (1979) **2015**, *347*, 425–428. [[CrossRef](#)] [[PubMed](#)]
214. Reyes, C.; Somogyi, R.; Niu, S.; Cruz, M.A.; Yang, F.; Catenacci, M.J.; Rhodes, C.P.; Wiley, B.J. Three-Dimensional Printing of a Complete Lithium Ion Battery with Fused Filament Fabrication. *ACS Appl. Energy Mater.* **2018**, *1*, 5268–5279. [[CrossRef](#)]
215. Chang, P.; Mei, H.; Zhou, S.; Dassios, K.G.; Cheng, L. 3D printed electrochemical energy storage devices. *J. Mater. Chem. A Mater.* **2019**, *7*, 4230–4258. [[CrossRef](#)]
216. Wei, M.; Zhang, F.; Wang, W.; Alexandridis, P.; Zhou, C.; Wu, G. 3D direct writing fabrication of electrodes for electrochemical storage devices. *J. Power Sources* **2017**, *354*, 134–147. [[CrossRef](#)]
217. Zhu, C.; Liu, T.; Qian, F.; Chen, W.; Chandrasekaran, S.; Yao, B.; Song, Y.; Duoss, E.B.; Kuntz, J.D.; Spadaccini, C.M.; et al. 3D printed functional nanomaterials for electrochemical energy storage. *Nano Today* **2017**, *15*, 107–120. [[CrossRef](#)]
218. Deiner, L.J.; Bezerra, C.A.G.; Howell, T.G.; Powell, A.S. Digital Printing of Solid-State Lithium-Ion Batteries. *Adv. Eng. Mater.* **2019**, *21*, 1900737. [[CrossRef](#)]
219. Zhang, F.; Wei, M.; Viswanathan, V.V.; Swart, B.; Shao, Y.; Wu, G.; Zhou, C. 3D printing technologies for electrochemical energy storage. *Nano Energy* **2017**, *40*, 418–431. [[CrossRef](#)]
220. Costa, C.M.; Gonçalves, R.; Lanceros-Méndez, S. Recent advances and future challenges in printed batteries. *Energy Storage Mater.* **2020**, *28*, 216–234. [[CrossRef](#)]
221. Fu, K.; Wang, Y.; Yan, C.; Yao, Y.; Chen, Y.; Dai, J.; Lacey, S.; Wang, Y.; Wan, J.; Li, T.; et al. Graphene Oxide-Based Electrode Inks for 3D-Printed Lithium-Ion Batteries. *Adv. Mater.* **2016**, *28*, 2587–2594. [[CrossRef](#)]
222. Yoshima, K.; Munakata, H.; Kanamura, K. Fabrication of micro lithium-ion battery with 3D anode and 3D cathode by using polymer wall. *J. Power Sources* **2012**, *08*, 404–408. [[CrossRef](#)]
223. Sun, K.; Wei, T.S.; Ahn, B.Y.; Seo, J.Y.; Dillon, S.J.; Lewis, J.A. 3D Printing of Interdigitated Li-Ion Microbattery Architectures. *Adv. Mater.* **2013**, *25*, 4539–4543. [[CrossRef](#)] [[PubMed](#)]
224. Yao, B.; Chandrasekaran, S.; Zhang, J.; Xiao, W.; Qian, F.; Zhu, C.; Duoss, E.B.; Spadaccini, C.M.; Worsley, M.A.; Li, Y. Efficient 3D Printed Pseudocapacitive Electrodes with Ultrahigh MnO₂ Loading. *Joule* **2019**, *3*, 459–470. [[CrossRef](#)]
225. Yao, B.; Chandrasekaran, S.; Zhang, H.; Ma, A.; Kang, J.; Zhang, L.; Lu, X.; Qian, F.; Zhu, C.; Duoss, E.B.; et al. 3D-Printed Structure Boosts the Kinetics and Intrinsic Capacitance of Pseudocapacitive Graphene Aerogels. *Advanced Materials* **2020**, *32*, 1906652. [[CrossRef](#)]
226. Shen, K.; Ding, J.; Yang, S. 3D Printing Quasi-Solid-State Asymmetric Micro-Supercapacitors with Ultrahigh Areal Energy Density. *Adv. Energy Mater.* **2018**, *8*, 1800408. [[CrossRef](#)]
227. Park, S.H.; Goodall, G.; Kim, W.S. Perspective on 3D-designed micro-supercapacitors. *Mater. Des.* **2020**, *193*, 108797. [[CrossRef](#)]
228. Zhang, Y.Z.; Wang, Y.; Cheng, T.; Yao, L.Q.; Li, X.; Lai, W.Y.; Huang, W. Printed supercapacitors: Materials, printing and applications. *Chem. Soc. Rev.* **2019**, *48*, 3229–3264. [[CrossRef](#)]
229. Huang, C.; Dontigny, M.; Zaghbi, K.; Grant, P.S. Low-tortuosity and graded lithium ion battery cathodes by ice templating. *J. Mater. Chem A Mater.* **2019**, *7*, 21421–21431. [[CrossRef](#)]
230. Fieber, L.; Evans, J.D.; Huang, C.; Grant, P.S. Single-operation, multi-phase additive manufacture of electro-chemical double layer capacitor devices. *Addit. Manuf.* **2019**, *28*, 344–353. [[CrossRef](#)]

231. Maurel, A.; Grugeon, S.; Fleutot, B.; Courty, M.; Prashantha, K.; Tortajada, H.; Armand, M.; Panier, S.; Dupont, L. Three-Dimensional Printing of a LiFePO₄/Graphite Battery Cell via Fused Deposition Modeling. *Sci. Rep.* **2019**, *9*, 18031. [[CrossRef](#)] [[PubMed](#)]
232. Pandolfo, T.; Ruiz, V.; Sivakkumar, S.; Nerkar, J. General Properties of Electrochemical Capacitors. *Supercapacitors* **2013**, *2*, 69–109. [[CrossRef](#)]
233. Zhang, C.; Chen, F.; Huang, Z.; Jia, M.; Chen, G.; Ye, Y.; Lin, Y.; Liu, W.; Chen, B.; Shen, Q.; et al. Additive manufacturing of functionally graded materials: A review. *Mater. Sci. Eng. A* **2019**, *764*, 138209. [[CrossRef](#)]
234. Tan, L.; Wang, G.; Guo, Y.; Fang, Q.; Liu, Z.; Xiao, X.; He, W.; Qin, Z.; Zhang, Y.; Liu, F.; et al. Additively manufactured oxide dispersion strengthened nickel-based superalloy with superior high temperature properties. *Virtual Phys. Prototyp.* **2020**, *15*, 555–569. [[CrossRef](#)]
235. Fricke, K.; Gierlings, S.; Ganser, P.; Venek, T.; Bergs, T. Geometry Model and Approach for Future Blisk LCA. *IOP Conf. Ser. Mater. Sci. Eng.* **2021**, *1024*, 012067. [[CrossRef](#)]
236. Wittig, N. Digitalization: Laser Metal Deposition—The Future of Spare Parts and Repairs for Industrial Steam Turbines. In *Volume 8: Microturbines, Turbochargers, and Small Turbomachines*; Steam Turbines; American Society of Mechanical Engineers: New York, NY, USA, 2018. [[CrossRef](#)]
237. Kelbassa, I.; Wohlers, T.; Caffrey, T. Quo vadis, laser additive manufacturing? *J. Laser Appl.* **2012**, *24*, 050101. [[CrossRef](#)]
238. Li, X.; Li, H.; Fan, X.; Shi, X.; Liang, J. 3D-Printed Stretchable Micro-Supercapacitor with Remarkable Areal Performance. *Adv. Energy Mater.* **2020**, *10*, 1903794. [[CrossRef](#)]
239. Cuoci, A.; Frassoldati, A.; Faravelli, T.; Ranzi, E. OpenSMOKE++: An object-oriented framework for the numerical modeling of reactive systems with detailed kinetic mechanisms. *Comput. Phys. Commun.* **2015**, *192*, 237–264. [[CrossRef](#)]
240. Hurt, C.; Brandt, M.; Priya, S.S.; Bhatelia, T.; Patel, J.; Selvakannan, P.R.; Bhargava, S. Combining additive manufacturing and catalysis: A review. *Catal. Sci. Technol.* **2017**, *7*, 3421–3439. [[CrossRef](#)]
241. Huang, F.; Wang, S.; Yi, W.; Zou, S.; Chen, C.; Xiao, L.; Liu, X.; Fan, J. Mix and print: Fast optimization of mesoporous CuCeZrO_w for catalytic oxidation of n-hexane. *Chem. Commun.* **2015**, *51*, 8157–8160. [[CrossRef](#)] [[PubMed](#)]
242. Kuang, X.; Wu, J.; Chen, K.; Zhao, Z.; Ding, Z.; Hu, F.; Fang, D.; Qi, H.J. Grayscale digital light processing 3D printing for highly functionally graded materials. *Sci. Adv.* **2019**, *5*, eaav5790. [[CrossRef](#)] [[PubMed](#)]
243. Achenbach, E. Heat and flow characteristics of packed beds. In *Experimental Heat Transfer, Fluid Mechanics and Thermodynamics*; Elsevier: Amsterdam, The Netherlands, 1993; pp. 283–293. [[CrossRef](#)]
244. Busse, C.; Freund, H.; Schwieger, W. Intensification of heat transfer in catalytic reactors by additively manufactured periodic open cellular structures (POCS). *Chem. Eng. Process.—Process Intensif.* **2018**, *124*, 199–214. [[CrossRef](#)]
245. Stuecker, J.N.; Miller, J.E.; Ferrizz, R.E.; Mudd, J.E.; Cesarano, J. Advanced Support Structures for Enhanced Catalytic Activity. *Ind. Eng. Chem. Res.* **2004**, *43*, 51–55. [[CrossRef](#)]
246. Lazarov, B.S.; Sigmund, O.; Meyer, K.E.; Alexandersen, J. Experimental validation of additively manufactured optimized shapes for passive cooling. *Appl. Energy* **2018**, *226*, 330–339. [[CrossRef](#)]
247. Hou, H.; Simsek, E.; Ma, T.; Johnson, N.S.; Qian, S.; Cissé, C.; Stasak, D.; Al Hasan, N.; Zhou, L.; Hwang, Y.; et al. Fatigue-resistant high-performance elastocaloric materials made by additive manufacturing. *Science (1979)* **2019**, *366*, 1116–1121. [[CrossRef](#)] [[PubMed](#)]
248. Klinar, K.; Kitanovski, A. Thermal control elements for caloric energy conversion. *Renew. Sustain. Energy Rev.* **2020**, *118*, 109571. [[CrossRef](#)]
249. Navickaitė, K.; Liang, J.; Bahl, C.; Wieland, S.; Buchenau, T.; Engelbrecht, K. Experimental characterization of active magnetic regenerators constructed using laser beam melting technique. *Appl. Therm. Eng.* **2020**, *174*, 115297. [[CrossRef](#)]
250. Moore, J.D.; Klemm, D.; Lindackers, D.; Grasemann, S.; Träger, R.; Eckert, J.; Löber, L.; Scudino, S.; Katter, M.; Barcza, A.; et al. Selective laser melting of La(Fe,Co,Si)₁₃ geometries for magnetic refrigeration. *J. Appl. Phys.* **2013**, *114*, 043907. [[CrossRef](#)]
251. Hou, H.; Finkel, P.; Staruch, M.; Cui, J.; Takeuchi, I. Ultra-low-field magneto-elastocaloric cooling in a multiferroic composite device. *Nat. Commun.* **2018**, *9*, 4075. [[CrossRef](#)]
252. Bjørk, R.; Bahl, C.R.H.; Smith, A.; Christensen, D.V.; Pryds, N. An optimized magnet for magnetic refrigeration. *J. Magn. Magn. Mater.* **2010**, *322*, 3324–3328. [[CrossRef](#)]
253. Hou, X.; Li, H.; Shimada, T.; Kitamura, T.; Wang, J. Effect of geometric configuration on the electrocaloric properties of nanoscale ferroelectric materials. *J. Appl. Phys.* **2018**, *123*, 124103. [[CrossRef](#)]
254. Miramontes, E.; Jiang, E.A.; Love, L.J.; Lai, C.; Sun, X.; Tsouris, C. Process intensification of CO₂ absorption using a 3D printed intensified packing device. *AIChE J.* **2020**, *66*, e16285. [[CrossRef](#)]
255. Stec, M.; Tatarczuk, A.; Więclaw-Solny, L.; Krótki, A.; Ściążko, M.; Tokarski, S. Pilot plant results for advanced CO₂ capture process using amine scrubbing at the Jaworzno II Power Plant in Poland. *Fuel* **2015**, *151*, 50–56. [[CrossRef](#)]
256. Yang, S.; Zhao, Y.F. Additive Manufacturing-Enabled Part Count Reduction: A Lifecycle Perspective. *J. Mech. Des.* **2018**, *140*, 031702. [[CrossRef](#)]
257. Knudsen, J.N.; Andersen, J.; Jensen, J.N.; Biede, O. Evaluation of process upgrades and novel solvents for the post combustion CO₂ capture process in pilot-scale. *Energy Procedia* **2011**, *4*, 1558–1565. [[CrossRef](#)]
258. Yeh, J.T.; Pennline, H.W.; Resnik, K.P. Study of CO₂ Absorption and Desorption in a Packed Column. *Energy Fuels* **2001**, *15*, 274–278. [[CrossRef](#)]

259. Wang, M.; Joel, A.S.; Ramshaw, C.; Eimer, D.; Musa, N.M. Process intensification for post-combustion CO₂ capture with chemical absorption: A critical review. *Appl. Energy* **2015**, *158*, 275–291. [[CrossRef](#)]
260. Fernandez, E.S.; Goetheer, E.L.; Manzolini, G.; Macchi, E.; Rezvani, S.; Vlugt, T.J. Thermodynamic assessment of amine based CO₂ capture technologies in power plants based on European Benchmarking Task Force methodology. *Fuel* **2014**, *129*, 318–329. [[CrossRef](#)]
261. Alexandersen, J.; Andreasen, C.S. A Review of Topology Optimisation for Fluid-Based Problems. *Fluids* **2020**, *5*, 29. [[CrossRef](#)]
262. Collins, I.L.; Weibel, J.A.; Pan, L.; Garimella, S.V. A permeable-membrane microchannel heat sink made by additive manufacturing. *Int. J. Heat Mass Transf.* **2019**, *131*, 1174–1183. [[CrossRef](#)]
263. Guo, H. Highly Thermally Conductive 3D Printed Graphene Filled Polymer Composites for Scalable Thermal Management Applications. *ACS Nano* **2021**, *15*, 6917–6928. [[CrossRef](#)]
264. Collins, I.L.; Weibel, J.A.; Pan, L.; Garimella, S.V. Evaluation of Additively Manufactured Microchannel Heat Sinks. *IEEE Trans. Compon. Packag. Manuf. Technol.* **2019**, *9*, 446–457. [[CrossRef](#)]
265. Dede, E.M.; Joshi, S.N.; Zhou, F. Topology Optimization, Additive Layer Manufacturing, and Experimental Testing of an Air-Cooled Heat Sink. *J. Mech. Des.* **2015**, *137*, 111403. [[CrossRef](#)]
266. Iradukunda, A.C.; Huitink, D.R.; Luo, F. A Review of Advanced Thermal Management Solutions and the Implications for Integration in High-Voltage Packages. *IEEE J. Emerg. Sel. Top. Power Electron.* **2020**, *8*, 256–271. [[CrossRef](#)]
267. Garimella, S.V.; Persoons, T.; Weibel, J.A.; Gektin, V. Electronics Thermal Management in Information and Communications Technologies: Challenges and Future Directions. *IEEE Trans. Compon. Packag. Manuf. Technol.* **2017**, *7*, 1191–1205. [[CrossRef](#)]
268. Sohrabian, M.; Vaseghi, M.; Khaleghi, H.; Dehrooyeh, S.; Kohan, M.S.A. Structural Investigation of Delicate-Geometry Fused Deposition Modeling Additive Manufacturing Scaffolds: Experiment and Analytics. *J. Mater. Eng. Perform.* **2021**, *30*, 6529–6541. [[CrossRef](#)]
269. Belfi, F.; Iorizzo, F.; Galbiati, C.; Lepore, F. Space Structures with Embedded Flat Plate Pulsating Heat Pipe Built by Additive Manufacturing Technology: Development, Test and Performance Analysis. *J. Heat Transf.* **2019**, *141*, 9. [[CrossRef](#)]
270. Comotti, C.; Regazzoni, D.; Rizzi, C.; Vitali, A. Additive Manufacturing to Advance Functional Design: An Application in the Medical Field. *J. Comput. Inf. Sci. Eng.* **2017**, *17*, 3. [[CrossRef](#)]
271. Meisel, N.A.; Woods, M.R.; Simpson, T.W.; Dickman, C.J. Redesigning a Reaction Control Thruster for Metal-Based Additive Manufacturing: A Case Study in Design for Additive Manufacturing. *J. Mech. Des.* **2017**, *139*, 10. [[CrossRef](#)]
272. Stephenson, K. A Detailed Five-Year Review of Medical Device Additive Manufacturing Research and its Potential for Translation to Clinical Practice. In Proceedings of the ASME 2015 International Design Engineering Technical Conferences and Computers and Information in Engineering Conference, Boston, MA, USA, 2–5 August 2015; American Society of Mechanical Engineers: New York, NY, USA, 2015.
273. Wang, Y. Applications of additive manufacturing (AM) in sustainable energy generation and battle against COVID-19 pandemic: The knowledge evolution of 3D printing. *J. Manuf. Syst.* **2021**, *60*, 709–733. [[CrossRef](#)]
274. Ali Saqib, M.; Abbas, M.S.; Tanaka, H. Sustainability and innovation in 3D printing: Outlook and trends. *Clean Technol. Recycl.* **2024**, *4*, 1–21. [[CrossRef](#)]
275. Oláh, J.; Aburumman, N.; Popp, J.; Khan, M.A.; Haddad, H.; Kitukutha, N. Impact of Industry 4.0 on Environmental Sustainability. *Sustainability* **2020**, *12*, 4674. [[CrossRef](#)]
276. Elbadawi, M.; Basit, A.W.; Gaisford, S. Energy consumption and carbon footprint of 3D printing in pharmaceutical manufacture. *Int. J. Pharm.* **2023**, *639*, 122926. [[CrossRef](#)] [[PubMed](#)]
277. Anderson, A.; Gallegos, S.; Rezaie, B.; Azarmi, F. Present and Future Sustainability Development of 3D Metal Printing. *Eur. J. Sustain. Dev. Res.* **2021**, *5*, em0168. [[CrossRef](#)]

Disclaimer/Publisher's Note: The statements, opinions and data contained in all publications are solely those of the individual author(s) and contributor(s) and not of MDPI and/or the editor(s). MDPI and/or the editor(s) disclaim responsibility for any injury to people or property resulting from any ideas, methods, instructions or products referred to in the content.